VOL. 28, NO. 1

APRIL 1954

Public Roads

A JOURNAL OF HIGHWAY RESEARCH

PUBLISHED BY
THE BUREAU OF
PUBLIC ROADS,
U. S. DEPARTMENT
OF COMMERCE,
WASHINGTON

On the Blue Ridge Parkway in Virginia

Public Roads

A JOURNAL OF HIGHWAY RESEARCH

Vol. 28, No. 1 *April 1954*

Published Bimonthly

Edgar A. Stromberg, *Editor*

BUREAU OF PUBLIC ROADS

Washington 25, D. C.

DIVISION OFFICES

No. 1. 718 National Savings Bank Bldg., Albany 7, N. Y.
Connecticut, Maine, Massachusetts, New Hampshire, New Jersey, New York, Rhode Island, and Vermont.

No. 2. 707 Earles Bldg., Hagerstown, Md.
Delaware, District of Columbia, Maryland, Ohio, Pennsylvania, Virginia, and West Virginia.

No. 3. 50 Seventh St., N. E., Atlanta 5, Ga.
Alabama, Florida, Georgia, Mississippi, North Carolina, South Carolina, Tennessee, and Puerto Rico.

No. 4. South Chicago Post Office, Chicago 17, Ill.
Illinois, Indiana, Kentucky, Michigan, and Wisconsin.

No. 5. Federal Office Bldg., Kansas City 6, Mo.
Iowa, Kansas, Minnesota, Missouri, Nebraska, North Dakota, and South Dakota.

No. 6. 502 U. S. Courthouse, Fort Worth 2, Tex.
Arkansas, Louisiana, Oklahoma, and Texas.

No. 7. 870 Market St., San Francisco 2, Calif.
Arizona, California, Nevada, and Hawaii.

No. 8. 753 Morgan Bldg., Portland 8, Oreg.
Idaho, Montana, Oregon, Washington, and Alaska.

No. 9. Denver Federal Center, Bldg. 40, Denver 2, Colo.
Colorado, New Mexico, Utah, and Wyoming.

IN THIS ISSUE

PUBLIC ROADS is sold by the Superintendent of Documents, Government Printing Office, Washington 25, D. C., at $1 per year (foreign subscription $1.25) or 20 cents per single copy. Free distribution is limited to public officials actually engaged in planning or constructing highways, and to instructors of highway engineering. There are no vacancies in the free list at present.

The printing of this publication has been approved by the Director of the Bureau of the Budget, January 5, 1952.

U. S. DEPARTMENT OF COMMERCE
SINCLAIR WEEKS, Secretary

BUREAU OF PUBLIC ROADS
FRANCIS V. du PONT, Commissioner

Use of Indices in Estimating Peak Rates of Runoff

BY THE HYDRAULICS RESEARCH BRANCH
BUREAU OF PUBLIC ROADS

Reported by
WILLIAM D. POTTER
Chief, Hydrology Section

Every highway bridge or drainage structure is designed for some estimated peak rate of runoff. If this estimate is too high, the cost of the structure will be excessive. On the other hand, if the estimate is too low, the cost of maintenance and replacement will be excessive. Somewhere between these extremes lies the most economical design.

Regardless of the procedures used to determine the frequency with which we can afford to have the capacity of our structures exceeded, the question arises as to how best to estimate peak rates of runoff for selected frequencies.

One of two general lines of procedure may be followed. The first of these was very popular at the beginning of the century and is still being followed by many highway departments today. It consists primarily of lumping the effects of the many variables that affect runoff into one all-embracing coefficient which is used in some unsubstantiated empirical formula to obtain a peak rate of runoff of unknown frequency. The computed peak rate is then used as the basis for the hydraulic design of our highway structures.

The second line of procedure, and the one with which this article is concerned, requires the measurement of the principal factors that affect runoff and the determination of their relations to the magnitude and frequency of peak rates. The problem of computing the size of bridge required to discharge a given flood safely once the peak runoff is estimated is beyond the scope of this article.

SINCE the turn of the century much hydrologic data have been collected by such agencies as the Soil Conservation Service, Geological Survey, and Weather Bureau. These data are now available in the form of physiographic and topographic maps, stream flow and precipitation measurements, and aerial photographs. By the use of sound statistical procedures these data may be analyzed to furnish reliable estimates of the magnitude and frequency of peak rates of runoff for use in the hydraulic design of highway structures.

It is true that the magnitude of any peak rate of runoff is the net result of innumerable hydrologic factors. Fortunately for engineers, however, the measurement of all of these many variables is not necessary to obtain reliable estimates of peak rates for selected frequencies from watersheds of a limited size range located in the same physiographic area.

For any such physiographic area and limited watershed and frequency ranges it should be possible to select three or four topographic, agronomic, or meteorologic indices that control to a considerable degree the peak rates of runoff that could be expected from watersheds within the physiographic area. It should be kept in mind, however, that these controlling indices may be different from those for any other physiographic area. Likewise, these indices may be different from those for other watersheds within the same physiographic area but differing in size ranges or in the selected frequencies of their runoff peaks. Even where the controlling indices are found to be the same for two physiographic areas, their relation to the resulting peak rate of runoff may not be the same for the two areas.

For these reasons, the relations developed for any one physiographic area should not be extrapolated beyond specified size or frequency limits nor should they be applied outside of the designated boundaries of the physiographic area. The results of statistical analyses made of peak rates of runoff from watersheds in two adjacent physiographic areas are presented here as partial verification of the foregoing statements. It is not within the scope of this article to include the detailed technical procedures [1] used, but rather to present the results of a sample study in a usable form and to demonstrate that the reliability of estimates may be greatly increased by an analysis of all available hydrologic data.

The two physiographic areas for which these analyses were made are the Allegheny-Cumberland Plateau and the Glaciated Sandstone and Shale Areas of New York, Pennsylvania, and Ohio. The relations established for both areas are applicable to mixed-cover watersheds ranging in size from 1,000 to 400,000 acres and for frequency of peak rates of runoff of from once in 10 to once in 50 years.

Conclusions

The conclusions that may be drawn from the statistical analyses of runoff from watersheds in the Allegheny-Cumberland Plateau and the Glaciated Sandstone and Shale Areas can be stated as follows:

1. The variation in the magnitude of 10-year peak rates of runoff among watersheds in a physiographic area can be satisfactorily explained by the selection of a limited number of readily attainable indices.
2. The indices that are applicable for one physiographic area are not necessarily those that explain the variations in peak rates of runoff from watersheds in some other area.
3. Even if these indices should be the same for two physiographic areas, their relation to the magnitude of peak rates of runoff would probably be different.
4. The application of the analytical procedures here developed to other physiographic areas would greatly increase the reliability of stream-flow estimates so essential for the safe and economical design of highway drainage structures.

Allegheny-Cumberland Plateau

The Allegheny-Cumberland Plateau is tentatively described by the Soil Conservation Service of the U. S. Department of Agriculture as follows:

The Allegheny-Cumberland Plateau, occupying 48,708,500 acres, is on the western slope of the Appalachian uplift. It extends westward from the Allegheny-Cumberland front where it passes through central Pennsylvania, western Maryland, eastern West Virginia, eastern Kentucky, eastern Tennessee, and north-central Alabama to the western edge where it merges into the central basin of Ohio and the Highland Rim of Kentucky, Tennessee, and Alabama. The eastern edge of the Plateau top is 2,500–3,500 feet above sea level with a few ridges or mountains extending to 3,800–4,000 feet. The western part is 1,000–1,500 feet above sea level. The Plateau along the eastern edge has somewhat flattened tops with deep narrow stream gorges. The western part is severely dissected into comparatively narrow ridges and V-shaped valleys along which the terrace and bottom lands have a limited development. The relief is gently undulating or rolling to hilly and steeply sloping with little flattish relief. It has a typical dendritic drainage pattern. The rock formations are mainly gray alternating beds of acid shale and sandstone with some thin-bedded limestone and calcareous shale of Carboniferous Age. These formations are resting in a clear-horizontal position. The slope of the formations is so gradual that except for a few minor anticlines and synclines it is not noticeable. The land is used as follows: 18.5 percent, cultivated;

[1] *Rainfall and topographic factors that affect runoff*, by W. D. Potter. Transactions of American Geophysical Union, vol. 34, No. 1, pp. 67-73, Feb. 1953.

15 percent, grassland; 50 percent, woodland; 8 percent, miscellaneous; and about 8.5 percent is in public ownership.

The climate is cool, temperate, and humid. Winters are cold; summers mild. Rainfall ranges from 40 to 50 inches. The frost-free season is 120 to 150 days in the high plateau, and 140 to 170 days from the northern to southern part. Due to steep relief the runoff is rapid in spite of the

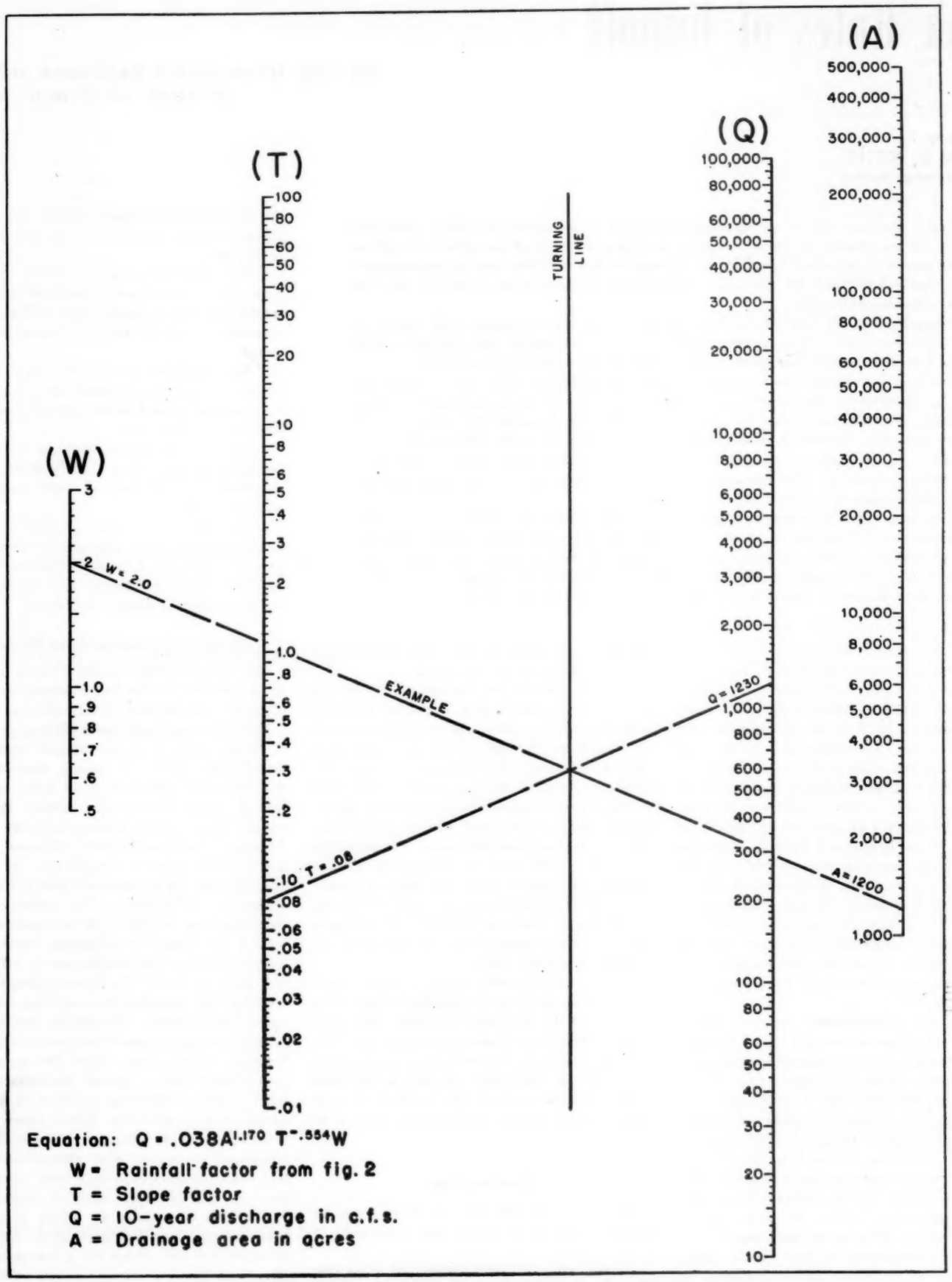

Figure 1.—Nomograph for discharge in the Allegheny-Cumberland Plateau.

large acreage of forest and grass cover. Original forest cover was oak, hickory, walnut, poplar, and maple with ash, beech, birch, and hemlock in gorges, spruce on high elevations, and pitch pine on southern reaches. A fairly large acreage is in National and State forests.

The soils are residual. Under forest cover they have a thin mat of organic matter on the surface more or less mixed at the bottom with mineral soil materials. This rests on brown to gray-brown mellow soil which passes at about 8 inches into a yellow-brown friable subsoil, passing at 24 to 48 inches into partly disintegrated parent material. Over extensive areas bedrock comes within the 3-foot soil profile. Soils contain much shaly, channery, and flaggy pieces of rock materials, and in places a noticeable amount of stone, usually sandstone.

Although there is still a considerable area in forest and wood lots, much of the land is cleared and used for general farming, dairying, stock-raising (beef cattle and sheep), and orcharding (apples). Under this system of farming, a large percentage of the land is in pasture. Crop yields are fairly good where manure, lime, and fertilizers are used. These practices are in common usage. The climatic differences from north to south in the stretch of some 800 miles are responsible for variations in the agriculture of the area.

Standard Error of Estimate

Simple correlation

For the area thus described by the Soil Conservation Service, peak-rate probability curves were computed for 51 mixed-cover watersheds ranging in size from 1,000 to 400,000 acres, based on runoff measurements of the U. S. Geological Survey and the Soil Conservation Service. The runoff record available for the majority of these watersheds was for the period 1938–48, and this short record was therefore selected for the computation of the probability curves. The average relation was determined between the 10-year peak rates and the corresponding watershed area. A statistical analysis showed that 67 times out of 100 the 10-year peak could be expected to vary from that indicated by this relation by as much as 35 percent. In other words, the standard error was 35 percent. This large standard error was evidence that the variation of 10-year peak rates could not be satisfactorily explained by consideration of area alone.

Multiple correlation

Three additional variables were selected, two of them indicative of the precipitation experienced during the short period of runoff record and the other indicative of topographic features. The precipitation indices were designated as the P and S ratios and were computed from U. S. Weather Bureau records for the period 1938–48. The P ratios were numerical expressions of the differ-

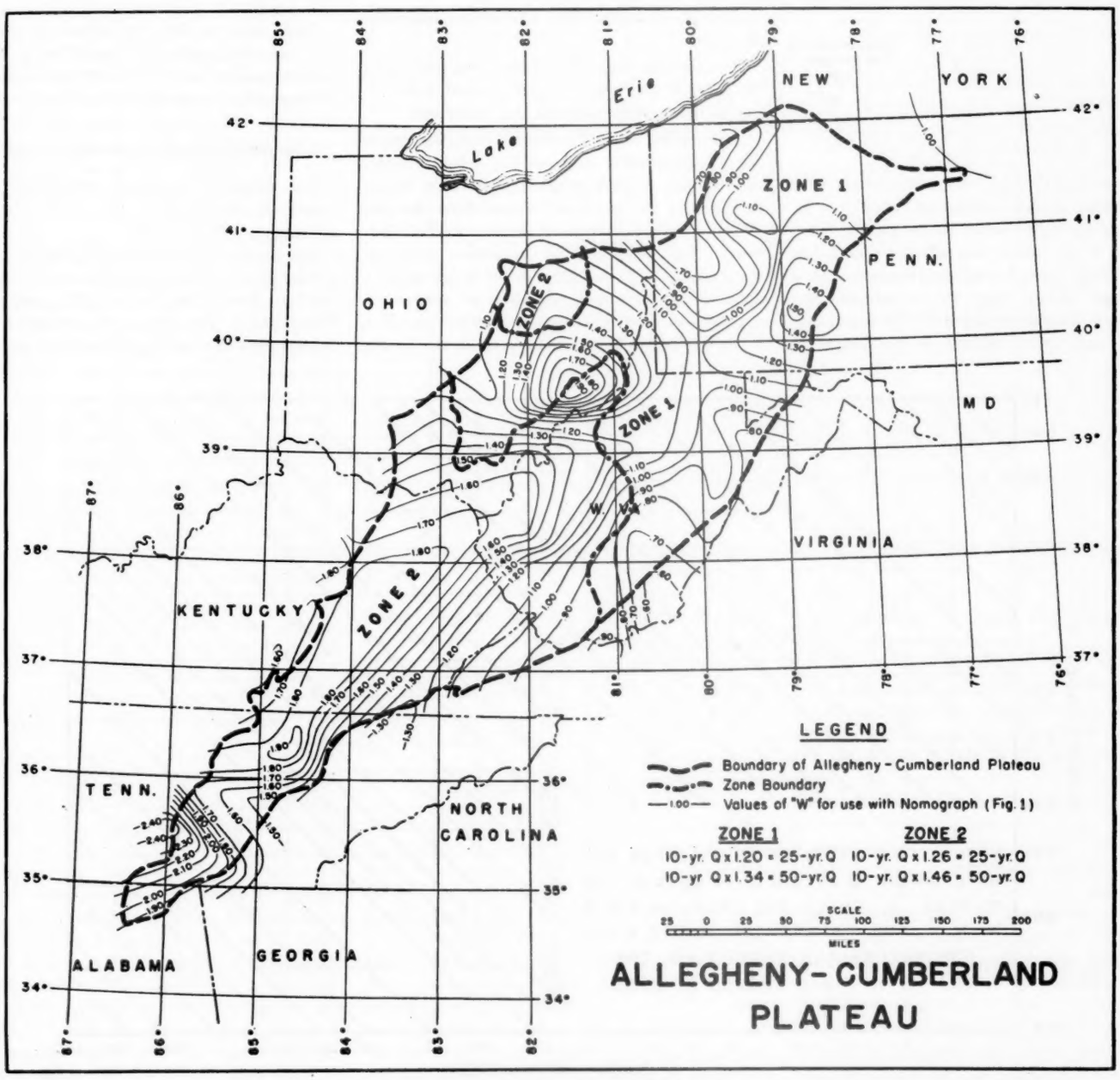

Figure 2.—Values of W for use with the nomograph (fig. 1) for discharge in the Allegheny-Cumberland Plateau.

ences in the intensity of precipitation among watersheds and the S ratio expressed the difference in annual precipitation and the number or frequency of excessive storms. The topographic index was designated as the T factor. It was computed from the topographic maps of the Geological Survey and when considered with area was indicative of differences in watershed shape, channel storage, and time of concentration.

A multiple correlation was then computed in which the watershed area A, the P ratio, the S ratio, and the T factor were considered as independent variables with the 10-year peak rate of runoff (q) as the dependent variable. A statistical analysis of the relations determined by this correlation showed that the standard error was 18 percent. In other words, the reliability with which 10-year peaks could be estimated 67 times out of 100 had been almost doubled over what it had been when area alone was considered. The progressive reduction in standard error as each new variable was introduced into the correlation is as follows:

	Standard error in percent
q vs. A	35
q vs. A and T	30
q vs. A, T, and P	21
q vs. A, T, P, and S	18

The 10-year peak rates used in this study were all predicated on short periods of runoff records. They could be indicative of future events, therefore, only if the factors that affected runoff during that short period were representative of a much longer period. Since the topographic factors of any watershed may be considered constant, the only factor affected by the length of the period of record would be precipitation. The precipitation indices P and S were, therefore, recomputed from Weather Bureau records covering the longer period 1915–48. The relations established for the short runoff period, as expressed by the regression equation, could then be utilized with these long-term precipitation indices to obtain new values of 10-year peak rates. These new values would be the peak rates that could have been expected from probability curves if the longer runoff record had been available.

Aids in Computing Peak Rates

To facilitate the solution of the regression equation a nomograph (fig. 1) and map (fig. 2) were prepared in which the two precipitation indices were combined in a single index W. To use these aids in estimating the peak rates of runoff that may be expected for a 10-, 25-, or 50-year recurrence interval, the procedure is as follows:

Area A.—Determine the area of the watershed in acres.

Precipitation index W.—Locate the watershed on figure 2 and select a precipitation index W that is the average value for that watershed.

Topographic index T.—From a U. S. Geological Survey topographic map, or any other accurate contour map of the watershed, measure the length in miles of the principal stream from the site of the proposed culvert or bridge to the headwater. The headwater, or uppermost point on the stream, should be taken as the point where a definite channel begins regardless of whether or not streamflow at this point is intermittent. If a U. S. Geological Survey map is used, the length of stream should include that portion shown as a broken blue line. Divide the length of the principal stream into two reaches, the lower reach being 0.7 of the total length and the upper reach the remaining 0.3. From the contours, determine the elevation of the stream channel at the upper and lower limits of each reach. Compute the average slope of each reach as the fall of the stream channel in feet divided by the length of channel in miles. Divide the length of stream channel for each reach measured in miles by the square root of the corresponding slope, and add the quotients. This sum is the topographic index T.

Use of nomograph.—Using the nomograph (fig. 1) and a straightedge, connect area A with rainfall factor W and mark the intersection with the turning line. Connect this intersection with the topographic factor T and extend the line to the Q scale. The intersection with the Q scale is the desired peak rate of runoff in cubic feet per second, for a 10-year recurrence interval (see example, fig. 1).

Peak rates for 25- and 50-year frequencies.—To obtain the peak rate of runoff for a 25- or 50-year frequency, multiply the 10-year peak by the corresponding coefficient (fig. 2).

Glaciated Sandstone and Shale Area

The Glaciated Sandstone and Shale Area is tentatively described by the Soil Conservation Service as follows:

The northern Appalachian Plateau or glaciated portion of the Appalachian Plateau is situated in southern New York, northern Ohio, and northern Pennsylvania. The plateau top, consisting of nearly level plains and rolling hills, ranges from 1,200–

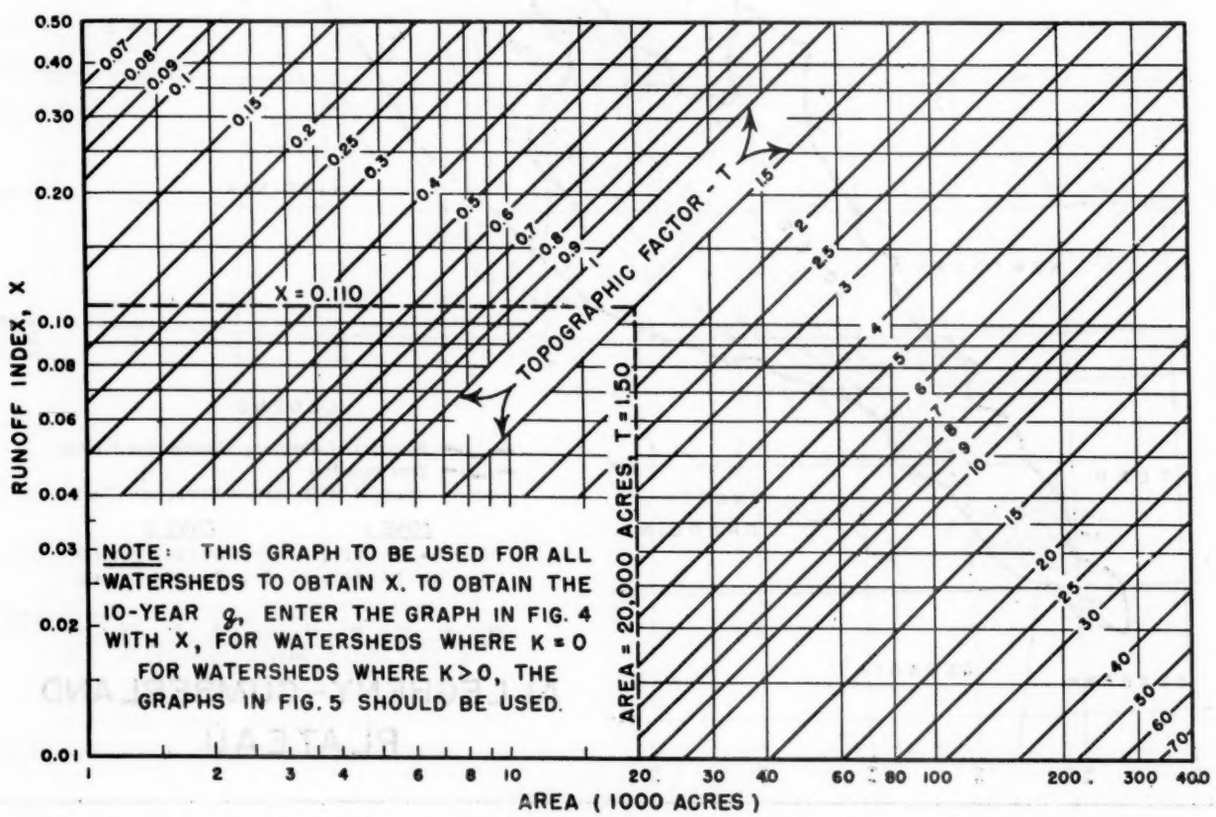

Figure 3.—Relation between area, topography, and runoff index for the Glaciated Sandstone and Shale Area.

1,500 feet in the western part to 1,800–2,500 feet in the eastern part. The geologic material consists of acid gray sandstone and shale over much of the area, with red sandstone and shales in the eastern part, and mixed alkaline and acid gray shales and sandstones, with some limestone material along the northern border. This is covered by drift from the Wisconsin glaciation consisting of bedrock material with little influence from outside sources.

This is essentially a "double-deck" country, consisting of a high plateau flattened to undulating to rolling, having fairly steep valley walls and fairly broad valleys filled with till and outwash material. The valley floors are about 1,000–1,200 feet below the general plateau level. A considerable area of the higher plateau is in forest and a lesser area of the remainder is forested.

The climate is cool, temperate, and humid. Winters are long and cold. Precipitation ranges from 35 to 50 inches from west to east. Frost-free period on the plateau top is 110 to 130 days and in the valleys about 2 to 3 weeks longer.

The soils on the higher plateau are moderately deep to shallow and at lower elevations they are somewhat deeper. Soils are generally medium-textured, with moderately heavy subsoils, and are mainly acid with some alkaline and calcareous materials. Some areas are poorly drained, but mainly they are excessively drained. The conservation problem is moderate to severe water erosion, but the main problem is controlling erosion on steep slopes. This is done mainly by strip cropping, permanent pasture, or reforestation. The land is used for general farming, dairying, and fruit growing. On the higher plateau the crops are hay, oats, buckwheat, and potatoes, and on the lower areas hay, corn, wheat, oats, potatoes, vegetables, and fruit. There is much abandoned land on the plateau, some of which is being reforested by Federal and State agencies, and some is being purchased for potato production and other private enterprise.

The total area is 23,550,000 acres. Of this, 1,325,000 acres or 5½ percent is publicly owned, usually in State forest and parks; 2,151,000 acres or 9 percent is miscellaneous; 3,768,000 acres or 16 percent is in private forest; and 15,909,000 acres or 68 percent is in farms. Of the land in farms, 46 percent is cropland; 26 percent is grassland (pasture); 20 percent is woodland; and 6 percent is all other farm land.

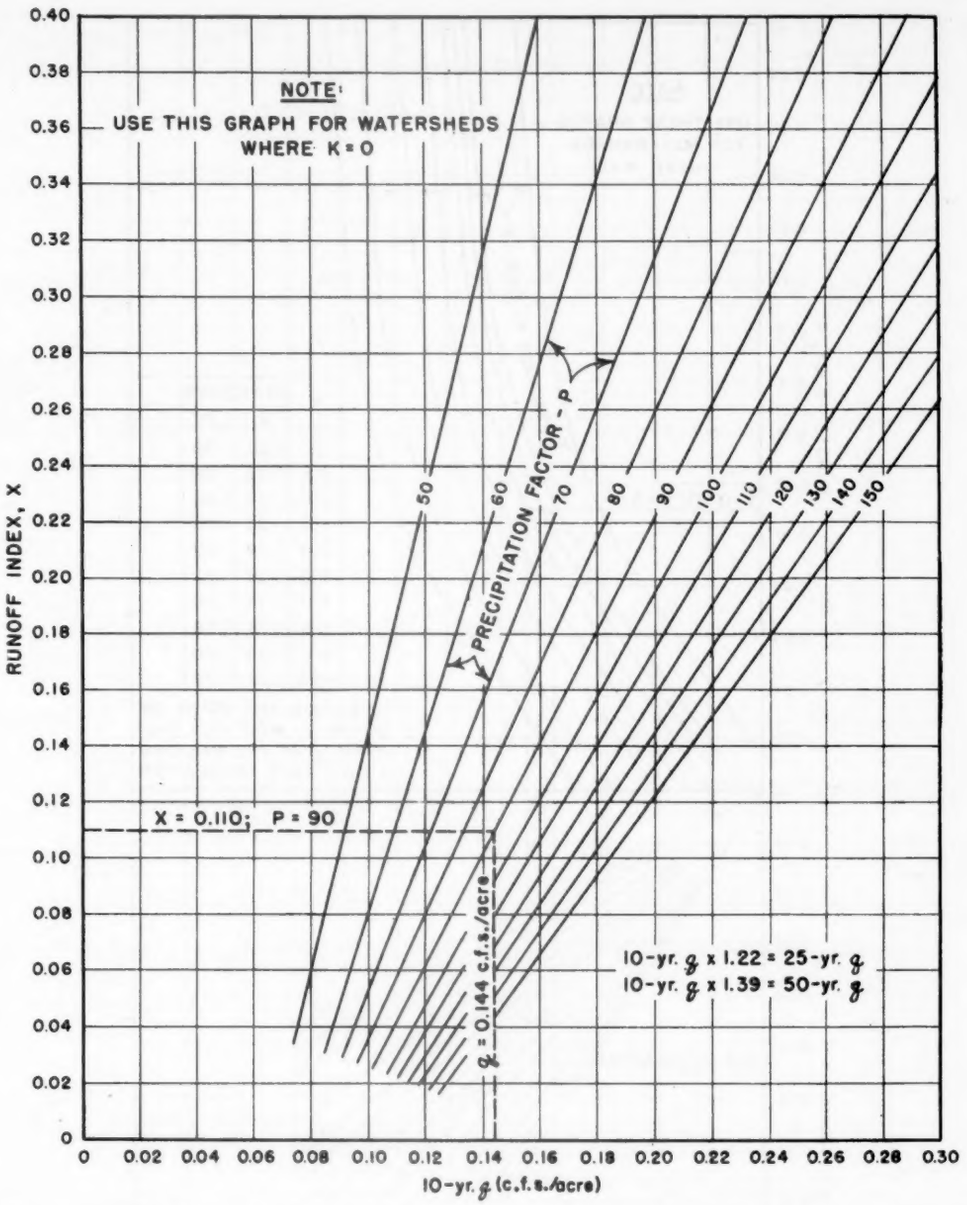

Figure 4.—Relation between runoff index, precipitation, and 10-year peak rate of runoff for the Glaciated Sandstone and Shale Area.

Relation of Two Variables

Following the same general procedure for the Glaciated Sandstone and Shale Area, thus described by the Soil Conservation Service, as that used in the case of the Allegheny-Cumberland Plateau, frequency curves were computed for the peak rates of runoff from 47 mixed-cover watersheds gaged by the U. S. Geological Survey and ranging in size from 1,000 to 400,000 acres. These probability curves were based on the short period of available runoff records starting with 1938 and extending through 1950. A statistical analysis of the average relation between the 10-year peak rate and the corresponding watershed area showed a standard error of 46 percent: that is, 67 times out of 100, the 10-year peak could be expected to vary from that indicated by this relation by as much as 46 percent. This large standard error led to the same conclusion as that made in the Allegheny-Cumberland study: that the variation of the 10-year peaks among watersheds could not be satisfactorily explained by consideration of area alone.

Additional Factors Considered

The two precipitation indices P and S, and the topographic index T, as described for the Allegheny-Cumberland Plateau, were computed for the Glaciated Sandstone and Shale Area. The precipitation indices were based on Weather Bureau records and were indicative of the precipitation experienced during the short period of runoff record. In addition, a new index K was selected to express the difference in runoff storage among watersheds. This storage was defined as the temporary or permanent storage occasioned by the presence of swamps, lakes, or reservoirs within the watershed or by the overflow of the lower reaches of the stream over all or part of its flood plain.

Graphical correlations (figs. 3–5) were made for the addition of each of these indices in which the 10-year peak rate (q) was taken as the dependent variable and the area of the watershed and the various indices as the independent variables. The standard error was computed for each correlation. For the 14 watersheds that had no runoff storage, it was found that the introduction of the topographic index T and the precipitation index P reduced the standard error of the correlation to 18 percent. No additional reduction was obtained by the further addition of the second precipitation index S. For the 33 watersheds that had runoff storage, however, the effect of the precipitation indices was reversed. The introduction of the topographic and storage indices T and K and the precipitation index S reduced the standard error to 18 percent, but no additional reduction was obtained by the further addition of the precipitation index P.

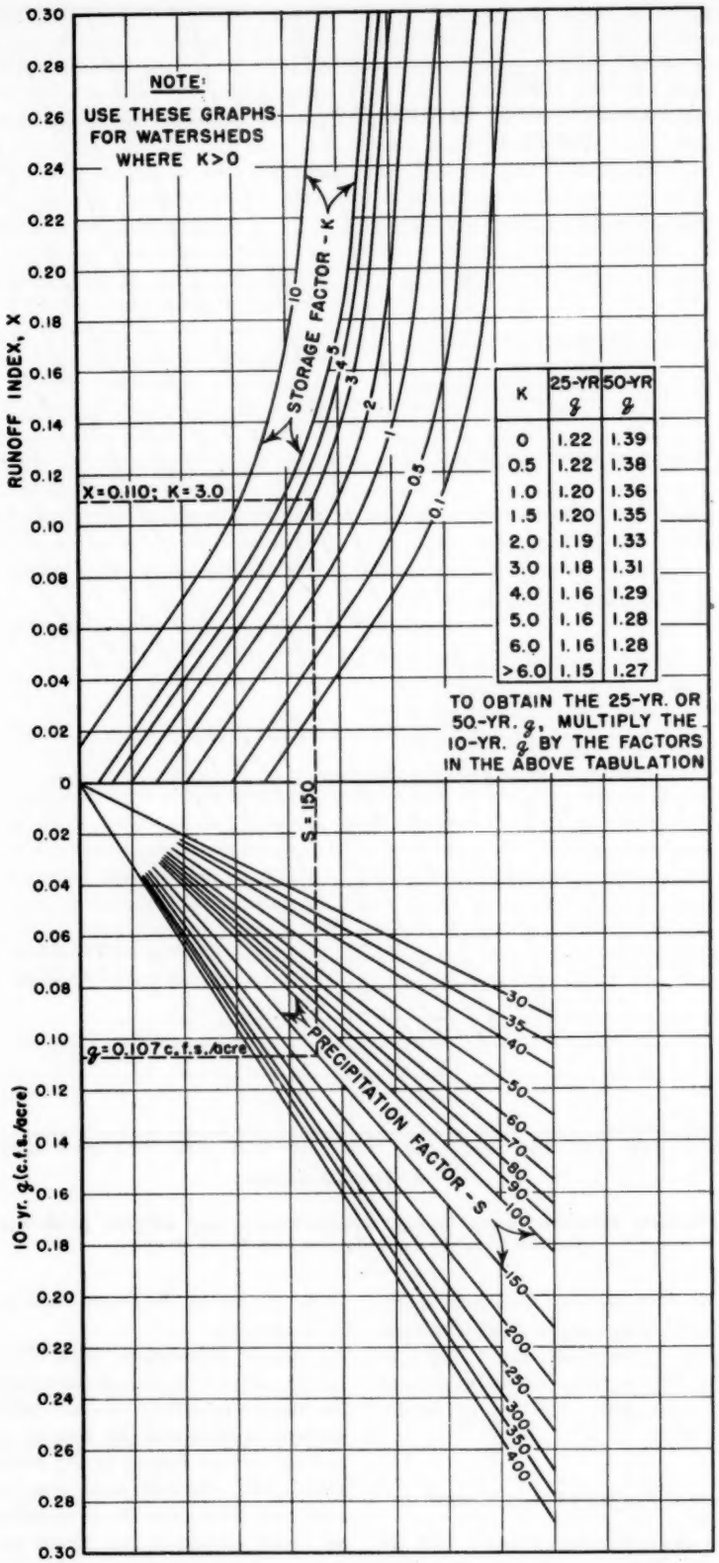

Figure 5.—Relation between runoff index, storage, precipitation, and 10-year peak rate of runoff for the Glaciated Sandstone and Shale Area.

As in the Allegheny-Cumberland Plateau, the reliability with which 10-year peaks could be estimated was materially increased by the consideration of topographic and precipitation indices. In the Glaciated Sandstone and Shale Area this increase in reliability was two-and-a-half times what it had been when area alone was considered. The progressive reduction in standard error as each new variable was introduced into the correlation is as follows:

	Standard error in percent
q vs. A	46
q vs. A and T	41
q vs. A, T, and K	24
q vs. A, T, K, and P or S	18

The relations established by the correlation graphs (figs. 3–5) for the short period of runoff record were utilized to obtain 10-year peak rates that would be representative of much longer periods. To do this it was necessary to recompute the precipitation indices from Weather Bureau records for the longer period 1915–50. Maps showing the areal variations of these long-term P and S indices (fig. 6) were prepared for use with the correlation graphs.

Maps and Graphs Utilized

To use these maps and correlation graphs in estimating peak rates of runoff that may be expected for a 10-, 25-, or 50-year recurrence interval, the procedure is as follows:

Area A.—Determine the area of the watershed in acres.

Topographic index T.—From a U. S. Geological Survey topographic map, or any other accurate contour map of the watershed, determine the topographic index T in the manner outlined for the Allegheny-Cumberland Plateau.

Storage index K.—From a U. S. Geological Survey topographic map, or any other accurate contour map of the watershed, measure the area of all swamps, lakes, or reservoirs. Also, where the average width of the valley bottom exceeds a quarter of a mile, a field inspection should be made to determine whether or not flooding of the valley is likely to occur. When flooding appears likely, a determination of the area that may be assumed to be covered by a 10-year flood should be made from the topographic map. For the purpose of use with the correlation graph (fig. 5), this flooded area should be taken as the total area of the valley bottom where its average width exceeds one quarter of a mile. Where railroads or major highways have been constructed on the valley bottom, it may be assumed that their embankments limit the extent of lateral flooding and they may be taken as one boundary of the flooded area. The sum of the areas of all swamps, lakes, reservoirs, and flood plains divided by the area of the watershed expressed in the same unit is the storage index K. (In measuring the areas, a considerable saving of time results from tracing the boundaries of these areas on tracing paper as one composite area which can then be planimetered in one operation.)

Precipitation index P.—If the storage index K for the watershed is zero, locate the watershed on figure 6 and select a precipitation index P that is the average value for that watershed.

Precipitation index S.—If the storage index K for the watershed is greater than zero, locate the watershed on figure 6 and select a precipitation index S that is the average value for that watershed.

Use of graphs.—To determine the 10-year peak rate of runoff, enter figure 3 with the watershed area and move vertically up the graph to the value on the T scale corresponding to that computed for the watershed. Move horizontally across the graph to the ordinate scale and record the indicated runoff index.

If the value of K for the watershed is zero, enter figure 4 with the runoff index and move horizontally across the graph to the value on the P scale corresponding to that selected for the water-

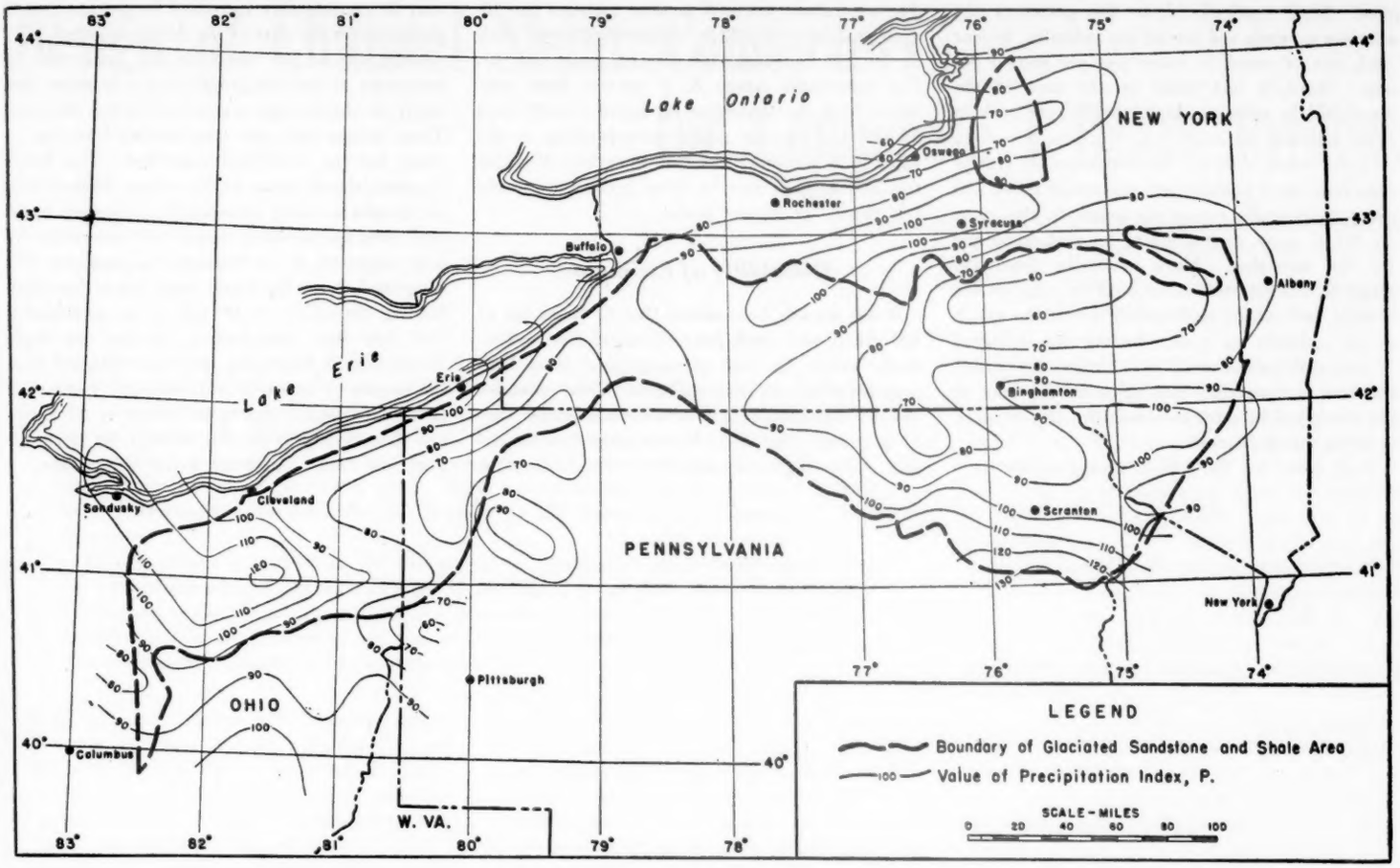

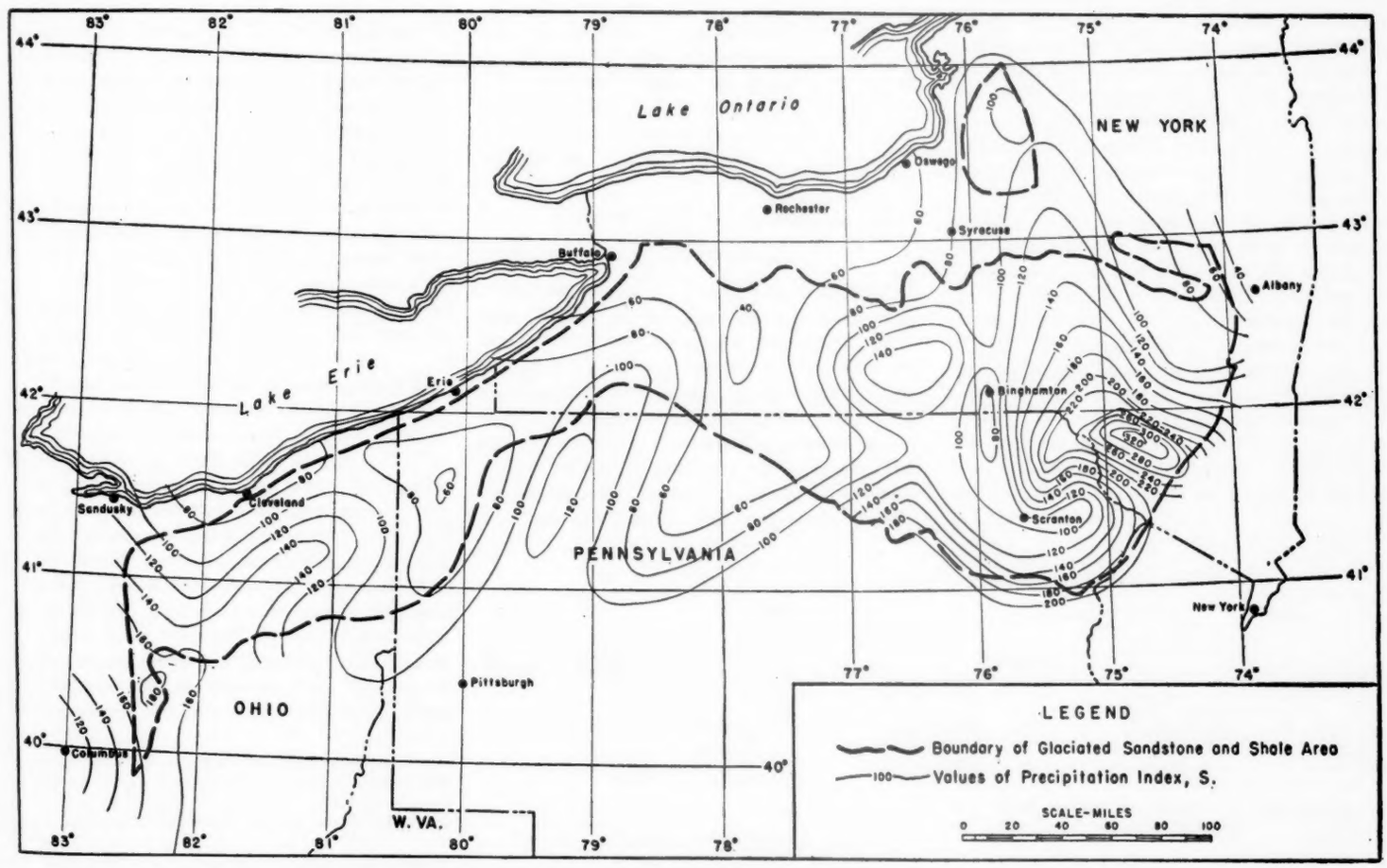

Figure 6.—Precipitation factors P (above) and S (below) for the Glaciated Sandstone and Shale Area.

shed. Move vertically down the graph to the abscissa q_{10} scale and record the indicated 10-year peak rate of runoff in cubic feet per second per acre. Multiply this value by the area of the watershed in acres to obtain the 10-year peak in cubic feet per second.

If the value of K for the watershed is greater than zero, enter figure 5 with the runoff index and move horizontally across the graph to the value on the K scale corresponding to that computed for the watershed. Move vertically down the graph to the selected value of S as read on the S scale and thence horizontally across the graph to the ordinate q_{10} scale. Record the indicated 10-year peak rate of runoff in cubic feet per second per acre and multiply this value by the area of the watershed in acres to obtain the 10-year peak in cubic feet per second.

Peak rates for 25- and 50-year frequencies.—For watersheds where K is zero, multiply the 10-year peak rate by 1.22 to obtain the 25-year peak or by 1.39 to obtain the 50-year peak (fig. 4). For watersheds where K is greater than zero, select from the tabulation on figure 5 coefficients for 25- and 50-year peaks corresponding to the value of K computed for the watershed. Multiply the 10-year peak rate by these coefficients to obtain the 25- or 50-year peak.

Reliability of Estimates

It has already been shown that 67 times out of 100 the 10-year peak rates of runoff from watersheds within the two physiographic areas here considered may be expected to vary from estimates derived through the use of the nomograph (fig. 1) or graphs (figs. 3–5) by not more than 18 percent. This degree of reliability of the estimates may be considerably increased by the exercise of judgment on the part of the design engineer. The descriptions of the physiographic areas are descriptions of the topography, soils, or cover that apply to the average watershed within the area. These factors may vary considerably from the average for any individual watershed. The design engineer should think of the values derived from the graphs as being bounded by 18-percent upper and lower bands within which he is to exercise his own judgment. If, for instance, an inspection of a watershed shows the depth (and hence the water-holding capacity) of the soil to be considerably less than that described as average, he might be justified in increasing the value obtained from the graphs by as much as 18 percent. Conversely if the soils were found to be deeper or more porous than described for the average, he might reduce the graph peaks by a like percentage.

Design of Channel Shear Connectors for Composite I-Beam Bridges

Reported by[1] IVAN M. VIEST, Research Assistant Professor of Theoretical and Applied Mechanics, and

CHESTER P. SIESS, Research Associate Professor of Civil Engineering, University of Illinois

In a composite I-beam bridge, a rigid connection between the concrete slab and the steel beams increases the stiffness of the bridge and permits use of smaller beams than would otherwise be required. The connection has a two-fold purpose—to prevent movement between the slab and the beams, and to transfer horizontal shear from one element to the other. Such a connection may be obtained by the use of channels welded to the top flanges of the beams and embedded in the concrete.

In this article a procedure for the design of flexible channel shear connectors for composite I-beam highway bridges is developed from data obtained in studies conducted at the University of Illinois. Equations are provided for use in the case of construction with shoring and also in the case of construction without shoring. The procedure is illustrated by an example.

BRIDGES composed of steel I-beams supporting a reinforced concrete slab may be built either with the slab resting freely on, or rigidly connected to, the beams. A rigid connection between the slab and the beams will increase considerably the stiffness of the bridge and, if considered in the design, will permit the use of a smaller I-section than would be required for a noncomposite design (ref. *3*).[2] In such a composite bridge the external loads are carried both by the beams and by the slab acting as a heavy flange of the steel beams. The necessary connection between the beams and the slab may be obtained by means of mechanical shear connectors attached to the top flange of the beams and embedded in the concrete of the slab. The twofold purpose of this connection is to prevent movement between the slab and the steel beams and to transfer horizontal shear from one element to the other.

Various types of shear connectors have been proposed and used. In general, they may be divided into three categories:

1. Rigid connectors such as square steel bars attached to the top flange of the I-beams;
2. Flexible connectors such as steel channels attached to the top flange of the I-beams;
3. Bond connectors such as reinforcement bars attached to the top flange of the I-beams in the form of loops or longitudinal helixes.

The flexible connector, made of a short piece of rolled steel channel with one flange welded to the beam and the other embedded in the slab, has been the subject of extensive experimental studies conducted at the University of Illinois in cooperation with the Illinois State Division of Highways and the Bureau of Public Roads (refs. *4, 6*). Numerous tests of individual connectors, as well as tests of composite beams with a series of connectors, have been made to obtain qualitative and quantitative data on the behavior of the connectors and on the influence of variations in the dimensions of the channel and the properties of the concrete on the load-carrying capacity of channel connectors.

In this article a procedure for the design of flexible channel shear connectors for composite I-beam highway bridges is developed on the basis of the data obtained from the Illinois tests. The procedure is illustrated by a numerical example on page 16.

Considerations for Design

Behavior of Composite T-beams

The advantages of a composite concrete and steel T-beam as compared to a noncomposite beam of the same dimensions are twofold: First, at a given load the deformations and therefore also the stresses in the composite structure are smaller; second, the ultimate load for the composite beam and the deflection at which the ultimate load is reached exceed substantially those for the noncomposite beam—in other words, the composite structure is tougher. The advantages of composite action are fully realized only if the shear connection is strong enough to prevent large slip between the I-beam and the slab and thus to insure full composite action at all levels of loading, up to the ultimate load. If, to the contrary, the shear connection permits large slip at the contact surfaces of the beam and the slab, the composite action is incomplete, the deformations at a given load are larger than in a fully composite structure of the same dimensions, and the ultimate load-carrying capacity is smaller. (Supporting experimental evidence can be found in refs. *4A, 6F*.)

In order to insure full benefit of the composite action, the design procedure presented in this article is based on the requirement of full composite action at all levels of loading. Such a procedure requires a knowledge of the ultimate flexural capacity of a composite T-beam.

The behavior of a composite steel and concrete T-beam subjected to a continuously increasing load may be divided into three stages. During the first stage, both the beam and the slab are elastic. The strain distribution and the stress distribution are approximately linear throughout the beam. The end of this stage is reached when the maximum stress in the beam reaches the yield-point value. During the second stage of loading, the yielding of the beam spreads upward into the web toward the top flange and along the bottom flange toward both supports, and the stresses in the slab enter the plastic range. The load increases throughout this stage of loading and the deformations increase at an increasing rate. At the end of this stage, the concrete slab fails by crushing in compression and the load-carrying capacity of the T-beam is thereby decreased considerably. If the load is allowed to decrease, the beam reaches a new equilibrium at a substantially lower load, and the third stage of loading follows.

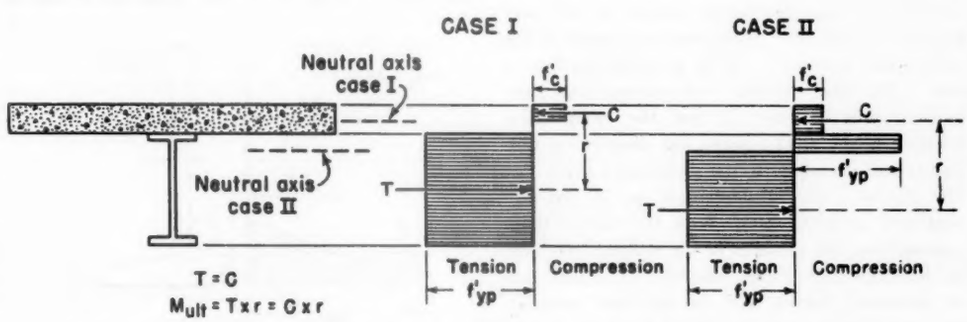

Figure 1.—Idealized distribution of stress in composite T-beam at ultimate load.

[1] This article is a report of an investigation conducted by the Engineering Experiment Station of the University of Illinois in cooperation with the Illinois State Division of Highways and the Bureau of Public Roads.

[2] Italic numbers in parentheses refer to the list of references on page 15.

NOTATION

A_c = Cross-sectional area of the portion of the concrete slab considered to act with the I-beam (*in.*²).

A_w = 0.707 weld size × weld length; effective area of the weld (*in.*²).

E_c = modulus of elasticity of concrete (*p.s.i.*).

E_s = modulus of elasticity of steel (*p.s.i.*).

$C_M = \frac{M_{DL}}{M_{LL}}$; $C_S = \frac{S_C}{S_I}$; $C_V = \frac{V_{DL}}{V_{LL}}$.

f'_c = compressive strength of concrete determined from the tests of 6 × 12-in. cylinders (*p.s.i.*).

f_{co} = maximum pressure on concrete adjacent to a channel shear connector (*p.s.i.*).

f_{max} = maximum steel stress in the web of a channel connector (*p.s.i.*).

f_s = allowable steel stress (*p.s.i.*).

f_{yp} = yield-point stress of steel in channels (*p.s.i.*).

f'_{yp} = yield-point stress of steel in beams (*p.s.i.*).

h = maximum thickness of channel flange (fig. 2) (*in.*).

h' = minimum thickness of channel flange (fig. 2) (*in.*).

I = moment of inertia of a composite T-beam computed from the area of the steel beam and the transformed area of the slab, A_c/n (*in.*⁴).

$k_1 = \frac{1.6}{\frac{f_{co}}{f'_c} + 1.8}$.

M_{ult} = resisting moment of a composite T-beam at ultimate load (fig. 1) (*in.-lb.*).

M_{DL} = maximum moment caused by the dead load (*in.-lb.*).

M_{LL} = maximum moment caused by the design live load, including impact (*in.-lb.*).

$n = E_s/E_c$.

Q = load on shear connector (*lb.*).

Q_{des} = design load on shear connector (*lb.*).

Q_{yp} = load on shear connector corresponding to first yielding of the connector (*lb.*).

Max. Q = the numerically largest load on a connector under moving design load (*lb.*).

Min. Q = the numerically smallest or the largest load of opposite direction to that of Max. Q on a connector under moving design load (*lb.*).

s = spacing of shear connectors (*in.*).

S_C = section modulus of a composite T-beam computed from the area of the steel beam and the transformed area of the slab, A_c/n (*in.*³).

S_I = section modulus of a steel I-beam (*in.*³).

S_{pl} = M_{ult}/f'_{yp}; plastic section modulus of a composite T-beam (corresponding to stress distribution shown in fig. 1) (*in.*³).

t = thickness of the web of a channel shear connector (fig. 2) (*in.*).

V = vertical shear on a composite T-beam (*lb.*).

V_{des} = maximum vertical shear on a composite T-beam at any point along the beam caused by the design load (*lb.*). In computing the design load for shear connectors (equation 7), $V_{des} = V_{LL}$ should be used for composite beams built without shoring and $V_{des} = V_{DL} + V_{LL}$ should be used for composite beams built with shoring.

V_{ult} = maximum vertical shear at any point along the beam caused by the ultimate flexural load (*lb.*).

V'_{ult} = maximum vertical shear on a composite T-beam at any point along the beam caused by the portion of the ultimate flexural load which contributes to the load acting on shear connectors (*lb.*). For a T-beam built without shoring, $V'_{ult} = V_{ult} - V_{DL}$; and for a T-beam built with shoring, $V'_{ult} = V_{ult}$.

V_{DL} = vertical shear at any point of the bridge caused by the dead load (*lb.*).

V_{LL} = maximum vertical shear at any point of the bridge caused by moving design live load, including impact (*lb.*).

w = length of a channel shear connector (*in.*).

y_c = distance between the center of gravity of the concrete slab and the neutral axis of the composite section (*in.*).

The beam carries the maximum load at the instant of crushing of the slab. The corresponding moment is called, in this article, the ultimate moment-carrying capacity of the T-beam. It has been shown by comparisons with the results of tests that the ultimate moment and load may be computed approximately on the assumption of the idealized distribution of stress shown in figure 1 (ref. *6G*). At this stage, the neutral axis of the composite section may be located either in the slab, case I in figure 1, or in the I-beam, case II in figure 1. It is assumed in both cases that the compressive stresses in the slab are uniformly distributed and equal to the concrete cylinder strength f'_c, and the tensile stresses in the steel I-beam are uniformly distributed and equal to the yield point stress f'_{yp}. It is assumed further in case I that the concrete slab cannot carry any tension, and in case II that the compressive stresses in the steel I-beam are distributed uniformly and are equal to the yield-point stress f'_{yp}. The effects of the reinforcement in the slab are neglected in both cases. With the aid of these assumptions, the position of the neutral axis may be determined from the condition of equilibrium of horizontal forces, and the ultimate moment-carrying capacity may be found from the condition of the equilibrium of moments (fig. 1).

Behavior of channel shear connectors

A cross-section of a flexible channel shear connector is shown in figure 2. The lower flange of the channel is connected rigidly to the I-beam and the entire connector is embedded in the concrete of the slab. When the connector is loaded, the lower flange, because of the rigid connection and stiffness, can neither bend nor rotate independently of the supporting beam. The flexible web deflects as a dowel. Accordingly, the distribution of pressure on the adjacent concrete is uniform adjacent to the stiff flange and nonuniform adjacent to the flexible web. The pressure distribution adjacent to the connector is shown in figure 2 as a dashed line. It can be seen that the pressure is concentrated at the end attached to the beam and that the magnitude of the pressure decreases rapidly with the distance from this end. At the upper end of the channel, both the pressure and the deflection or rotation of the web are usually so small that the conditions at this end may be neglected in discussing the behavior of a channel connector.

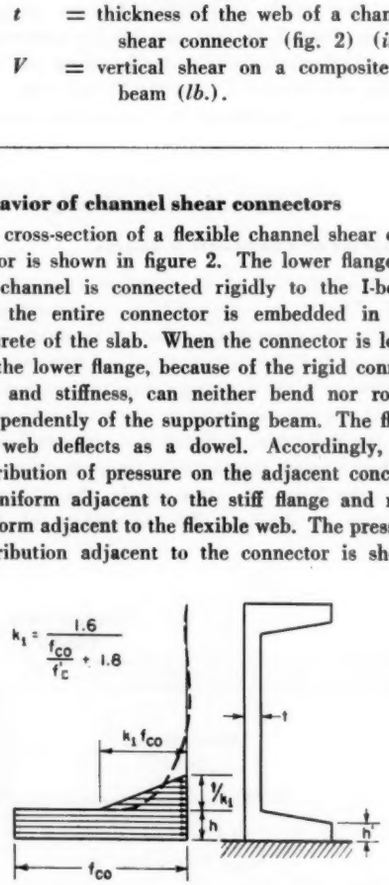

Figure 2.—Distribution of load on channel.

When the load is applied to a channel connector, the connector exerts pressure on the adjacent concrete. The connector is deformed and the concrete is compressed. The result of compressing the concrete is a relative movement between the slab and the connector and, in turn, a movement between the slab and the beam. The pressure distribution diagram indicates that the relative movement of the connector is largest at the lower flange (fig. 2). The movement of the lower flange is accompanied by deformations of the web. As those deformations are limited to sections of the web located close to the lower flange, the total deflection of the web at the junction with the lower flange must necessarily remain small as long as the stresses in the channel are elastic, or until crushing of the concrete permits the web to deform over a greater length. Thus as long as the steel of the connector does not yield and the

concrete of the slab does not crush, the relative movement between the channel and the slab, and therefore also the slip between the beam and the slab, remain small.

Critical stress

The maximum stress in a channel connector, f_{max}, is located at the junction of the lower flange and the web, and the maximum pressure on the concrete, f_{co}, is located adjacent to the lower flange of the channel. The magnitude of these maximum stresses may be evaluated with the aid of the idealized equivalent pressure distribution shown in figure 2 as a cross-hatched area.

The total pressure on the concrete must be equal to the load Q acting on the connector. It follows from figure 2 that the maximum pressure on the concrete is:

$$f_{co} = \frac{Q}{(h + \frac{1}{2}t)\, w} \qquad (1)$$

If the connector is considered to be a cantilever fixed at its lower end and loaded with the cross-hatched area, the maximum stress in the connector is:

$$f_{max} = \frac{Q}{k_1 (h + \frac{1}{2}t)\, w} \qquad (2)$$

where:

$$k_1 = \frac{1.6}{\frac{f_{co}}{f'_c} + 1.8} \qquad (3)$$

The quantity k_1 is an empirical coefficient evaluated from the tests of channel shear connectors. (Equations 1 and 2 were obtained originally by simplification of more complex theoretical formulas. Ref. *6D*).

It has been explained in the preceding discussion that the slip between the slab and the beam of a composite T-beam will be small as long as the stresses in the channel remain in the elastic range and the concrete does not crush. Thus the limiting stress for the steel is the yield-point stress and the limiting pressure for the concrete is that which causes crushing.

Only the concrete adjacent to the lower flange of the channel is subjected to high pressure. This high pressure is localized on a very small area of the slab so that the concrete at this location is in a state of confined compression. It is known that concrete under such state of stress can resist stresses appreciably greater than its cylinder strength. Furthermore, the magnitude of this pressure depends on the deformation of the channel web. Since the deformations of the web are small until the commencement of yielding of the steel, it seems unlikely that crushing of the concrete would occur before the connector has yielded.

The tests of channel shear connectors have shown conclusively that yielding occurs before crushing of the concrete. In all tests of individual shear connectors, the load causing first yielding of the channel was reached without any visible signs of distress in the concrete (ref. *6B*). Furthermore, the maximum test loads on all specimens were substantially higher than the loads at first yielding of the channels (table 1), and in most specimens no apparent signs of distress in the concrete could be observed in the vicinity of the region of high compressive stresses even at the maximum loads (ref. *6C*). Thus the critical stress for an individual shear connector is the yield-point stress, and the corresponding limiting load-carrying capacity of a shear connector may be computed from equation 2.

Table 1.—Load capacity of channel shear connectors beyond first yielding of connectors [1]

Channel size	Concrete strength	$\frac{Q_{ult}}{Q_{yp}}$
	P.s.i.	
3-in., 4.1-lb.	3,310	2.98
4-in., 5.4-lb.	2,070	2.57
4-in., 5.4-lb.[2]	2,810	2.48
4-in., 5.4-lb.	6,320	2.96
4-in., 5.4-lb.[3]	2,650	2.36
4-in., 7.25-lb.	2,300	2.06
4-in., 7.25-lb.	5,050	3.26
4-in., 7.25-lb.[3]	2,170	1.76
4-in., 13.8-lb.	2,670	2.21
5-in., 6.7-lb.	3,260	2.62

[1] Loads Q_{ult} and Q_{yp} on shear connectors measured in the test of push-out specimens (ref. *6A*).
[2] Connector was 4 inches long; all other connectors were 6 inches long.
[3] Specimen had a concrete fillet between the I-beam and the slab.

Conclusions

Two major conclusions may be drawn from the investigations which are the basis for the preceding discussions:

1. In a composite steel and concrete T-beam, it is desirable that full composite action be retained at all levels of loading, up to the ultimate load.

2. If the shear connection consists of flexible channel shear connectors, full composite action will be retained as long as the stresses in the connectors do not exceed the yield point.

Any procedure for the design of channel shear connectors based on these two requirements must necessarily be an ultimate design procedure, since it requires an evaluation of the capacity of the connectors corresponding to the ultimate moment-carrying capacity of the T-beam. Nevertheless, since current procedures for the design of I-beam bridges are based on working stresses and not on ultimate capacity, it is desirable to base the design of connectors also on working stresses. This can be done by modifying the ultimate design equations through the use of certain conversion factors, as shown in the following paragraphs.

Load Capacity of Channel Shear Connectors

Capacity at ultimate load on beam

When the load applied to a composite T-beam reaches the full moment capacity of the beam, the maximum steel stress in the connectors should not exceed the yield-point stress:

$$f_{max} = f_{yp} \qquad (4)$$

The load on the shear connectors at this stage may be found from equation 2 by substituting from equations 4, 3, and 1 for f_{max}, k_1, and f_{co}:

$$\frac{Q_{yp}}{(h + \frac{1}{2}t)\, w f'_c} = -0.9 + \sqrt{0.81 + 1.6 \frac{f_{yp}}{f'_c}} \qquad (5)$$

Equation 5 is shown graphically as a solid line in figure 3, in which the quantity on the left side of the equation is plotted against the ratio f_{yp}/f'_c. For structural steel with a specified yield-point stress of 33,000 p.s.i., and for concretes having compressive strengths varying from 2,500 to 5,000 p.s.i., the ratio f_{yp}/f'_c varies from 6.6 to 13.2. Within this range, which represents most practical conditions, equation 5 may be replaced by the simpler expression:

$$\frac{Q_{yp}}{(h + \frac{1}{2}t)\, w f'_c} = \sqrt{\frac{f_{yp}}{f'_c}} \qquad (6)$$

Equation 6 is shown in figure 3 as a broken line. It can be seen that within the practical range of values for f_{yp}/f'_c the maximum difference between the loads given by equations 5 and 6 is less than 5 percent, and for a range of f_{yp}/f'_c from 5.5 to 30 (corresponding to f_{yp} between 33,000 and 60,000 p.s.i., and f'_c between 2,000 and 6,000 p.s.i.) the maximum difference is less than 10 percent. For the common value of $f_{yp}/f'_c = 9.43$ ($f_{yp} = 33{,}000$ p.s.i., $f'_c = 3{,}500$ p.s.i.) the two equations yield practically identical results.

The loads computed from equation 6 are compared with the results of tests of individual shear connectors (ref. *6A*) in figure 4. The computed loads were obtained from equation 6 for $f_{yp} = 33{,}000$ p.s.i. and for the actual concrete cylinder strengths for the particular specimens. The meas-

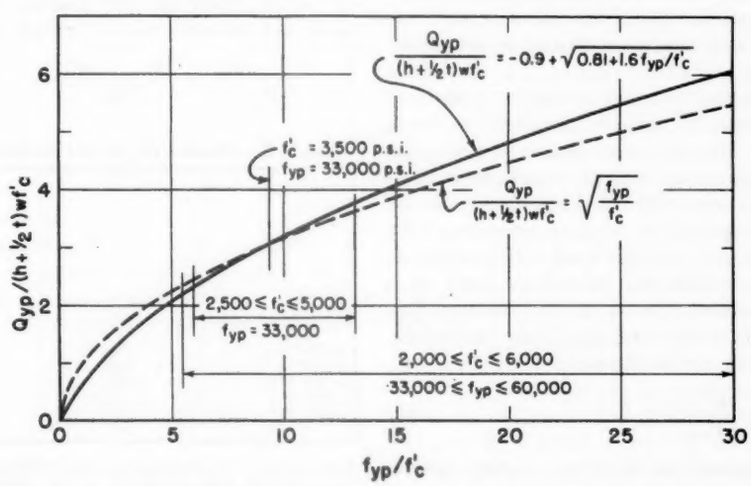

Figure 3.—Variation of yield capacity of channel connectors with ratio f_{yp}/f'_c.

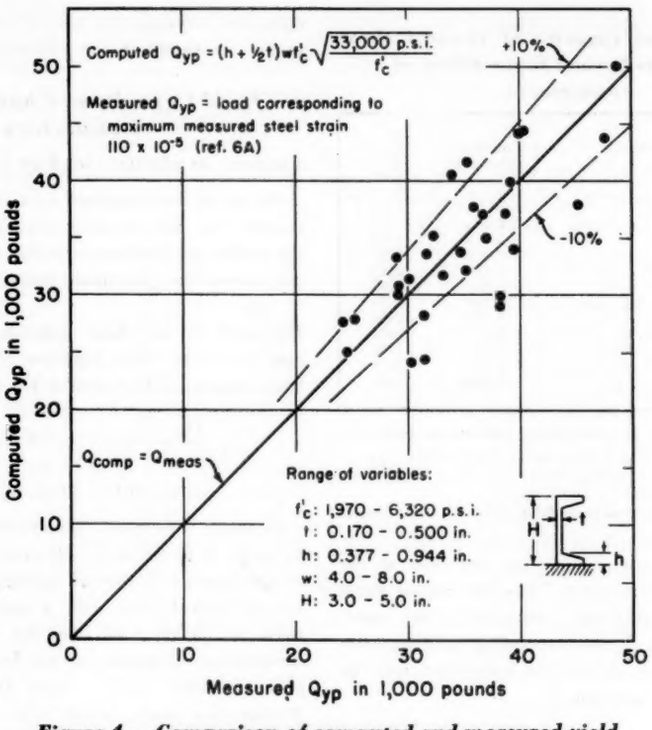

Figure 4.—Comparison of computed and measured yield capacities of channel connectors.

ured loads are those giving a measured maximum strain in the connector web of 110 × 10^{-5}, corresponding to a stress of 33,000 p.s.i. In spite of the wide range of variables included in this figure, all data group well around the line representing $Q_{measured} = Q_{computed}$.

Capacity at design load

If it is assumed that the connection between the beam and the slab of a composite T-beam is furnished only by the individual connectors, the load on any connector is the product of the horizontal shear per unit length of the beam and the spacing s of the connectors. As long as the stress distribution in the T-beam is elastic, the load on a connector may be computed from the equation:

$$Q = \frac{V A_c y_c}{n I} s \qquad (7)$$

If a portion of the beam has yielded, equation 7 gives approximately correct values of the loads acting on shear connectors located at sections of the T-beam at which yielding did not occur, whereas the load is somewhat higher on the connectors located at sections at which the beam has yielded. However, overstressing of a few connectors is not critical from the standpoint of composite action (ref. *6H*). Thus equation 7 may be used for computing the loads on connectors both at working and ultimate loads. This makes it possible to compute the ratio of the loads on a connector at first yielding of the connector, Q_{yp}, to that at the design load, Q_{des}, as the ratio of the corresponding vertical shears:

$$\frac{Q_{yp}}{Q_{des}} = \frac{V'_{ult}}{V_{des}} \qquad (8)$$

If it is desired that the factor of safety against first yielding of shear connectors be at least equal to the factor of safety of the composite T-beam against ultimate load, the magnitude of the ratio in equation 8 may be evaluated from the moment capacities of the T-beam at ultimate and at design loads. The relation between the shears and moments is different for beams built without temporary supports and for beams built with temporary supports. Therefore these two cases will be treated separately.

Beams without shoring

If a composite T-beam is built without any temporary supports, the steel I-beam must carry both its own dead load and the weight of the slab. Thus the shear connectors are required to resist only the live loads, and equation 8 may be written in the following form:

$$\frac{Q_{yp}}{Q_{des}} = \frac{V_{ult} - V_{DL}}{V_{LL}} \qquad (9)$$

It can be shown that the relation between the shear and moments may be written as:

$$\frac{V_{ult} - V_{DL}}{V_{LL}} = \frac{M_{ult} - M_{DL}}{M_{LL}} \qquad (10)$$

By definition:

$$M_{ult} = S_{pl} f'_{yp} \text{ and } M_{LL} = S_c f_s \cdot \frac{1}{1 + \frac{S_c M_{DL}}{S_I M_{LL}}}.$$

Also:

$$\frac{M_{DL}}{M_{LL}} = C_M \quad \text{and} \quad \frac{S_c}{S_I} = C_S.$$

If these expressions are substituted into equations 10 and 9, the ratio of loads on a shear connector may be expressed in the form:

$$\frac{Q_{yp}}{Q_{des}} = \frac{S_{pl}}{S_c} \frac{f'_{yp}}{f_s} (1 + C_S C_M) - C_M \qquad (11)$$

For structural steel for highway bridges, f_s = 18,000 p.s.i. and f'_{yp} = 33,000 p.s.i. The ratio of the plastic to the elastic section modulus, S_{pl}/S_c, depends on the dimensions of the slab and the beam, on the ratio n of the moduli of elasticity of steel and concrete, on the cylinder strength of the concrete, and on the yield-point stress of the steel beams. The magnitude of this ratio has been computed for a wide range of standard wide-flange beams of structural steel combined with concrete slabs of various sizes and strengths.

Representative results of these studies are presented in table 2. It can be seen that for T-beams in which the compressive stresses at ultimate are carried by the slab alone, that is, the neutral axis lies above the top flange of the steel beam (case I in fig. 1), the ratio S_{pl}/S_c varies approximately from 1.38 to 1.49. For T-beams in which the neutral axis at ultimate intersects the steel section, that is, the steel beam is not used to full tensile capacity because a portion of the compressive forces has to be resisted by the steel beam (case II in fig. 1), the value of the ratio S_{pl}/S_c decreases with decreasing contribution of the slab to the resisting compressive forces. The lower limit for this case is a steel I-beam without any slab, for which the ratio S_{pl}/S_c varies approximately from 1.10 to 1.20, depending on the proportions of the I-beam section. In most practical applications, the relative proportions of the slab

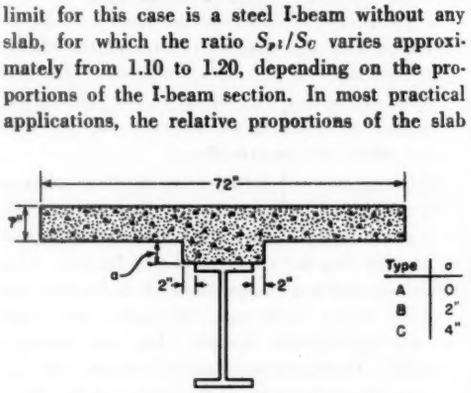

Figure 5.—Cross section (see table 2).

Table 2.—Ratios of plastic section moduli to elastic section moduli for composite T-beams

Beam	S_{pl}/S_c (f'_{yp} = 33,000 p.s.i.)				
	Cross-section type A,[1] f'_c as given below			Type B,[1] f'_c = 3,000 p.s.i.	Type C,[1] f'_c = 3,000 p.s.i.
	2,000 p.s.i.	3,000 p.s.i.	5,000 p.s.i.		
16WF36	1.48	1.45	1.38	1.45	1.42
21WF73	1.48	1.47	1.46	1.49	1.49
30WF116	[2] 1.37	1.42	1.44	1.45	1.47
36WF150	[2] 1.35	1.39	1.42	1.48	1.45
36WF300	[2] 1.26	[2] 1.29	[2] 1.32	[2] 1.30	[2] 1.30

[1] See figure 5 for cross-section dimensions.
[2] At ultimate load a portion of the compressive forces is resisted by the steel I-beam (fig. 1, case II); in all other cases all compression is resisted by the slab (fig. 1, case I).

and the I-beam will be such that at ultimate load the neutral axis will be located in the slab. Thus the ratio S_{p1}/S_c will vary within relatively narrow limits and may be replaced in equation 11 by a value of 1.45 without introducing any serious error.

If the shear connectors are made of structural steel, that is $f_{vp} = 33{,}000$ p.s.i. and if, in addition, $f'_{vp} = 33{,}000$ p.s.i. and $f_s = 18{,}000$ p.s.i., and if Q_{vp} is substituted from equation 6, then equation 11 may be written in the following form:

$$\frac{Q_{des}}{(h + \tfrac{1}{2}\,t)\; w\, f'_c} = \frac{1}{0.8 + (0.8\, C_S - 0.3)\; C_M}\sqrt{\frac{3000 \text{ p.s.i.}}{f'_c}} \quad (12)$$

Equation 12 is a design formula for channel shear connectors for beams built without shores. For any particular composite T-beam the quantities C_M, C_S, and f'_c are assumed to be known in advance of the design of shear connectors, and the right-hand side of equation 12 is therefore known. To simplify the use of equation 12, values of $(h + \frac{1}{2}\,t)$ for the steel channels now being rolled are listed in table 3. Because of the assumptions made in its derivation, and because of the limits of the experimental evidence on which it is based, equation 12 is applicable only to flexible channel shear connectors made of rolled channels of structural steel attached to rolled wide-flange I-beams, also of structural steel. It is applicable only to channels at least 3 inches deep and having a length w not less than six times the maximum thickness of the channel flange h (ref. *6E*).

Beams with shoring

If a composite T-beam is built with temporary supports, both the dead load and the live load are carried by the composite section and the shear connectors must resist both dead and live load. Equation 8 may then be written as:

$$\frac{Q_{vp}}{Q_{des}} = \frac{V_{ult}}{V_{LL} + V_{DL}} \quad (13)$$

The relation between the shear and the moments may be expressed as:

$$\frac{V_{ult}}{V_{LL} + V_{DL}} = \frac{\dfrac{M_{ult}}{M_{LL} + M_{DL}}(1 + C_M) - C_M + C_V}{1 + C_V} \quad (14)$$

where:

$$C_M = \frac{M_{DL}}{M_{LL}} \text{ and } C_V = \frac{V_{DL}}{V_{LL}}.$$

By definition, $M_{ult} = S_{p1} f'_{vp}$ and $(M_{LL} + M_{DL}) = S_c f_s$. Thus equation 13 may be written as:

$$\frac{Q_{vp}}{Q_{des}} = \frac{\dfrac{S_{p1}}{S_c}\dfrac{f'_{vp}}{f_s}(1 + C_M) - C_M + C_V}{1 + C_V} \quad (15)$$

and for beams and shear connectors made of structural grade steel the equation for the design load is:

$$\frac{Q_{des}}{(h + \tfrac{1}{2}\,t)\; w f'_c} = \frac{1 + C_V}{0.8 + 0.5\, C_M + 0.3\, C_V}\sqrt{\frac{3{,}000 \text{ p.s.i.}}{f'_c}} \quad (16)$$

For any particular composite T-beam, C_M is a constant but C_V varies from point to point along the span. Thus the use of equation 16 would result in a rather cumbersome design. However, the design procedure would become much more simple if the variable parameter C_V could be replaced by a constant. It can be shown that for $C_V = 0$, which represents the lowest possible value of C_V, equation 16 yields the minimum values of Q_{des}. Accordingly, the following equation will yield a conservative value of Q_{des} for composite T-beams built with shoring:

$$\frac{Q_{des}}{(h + \tfrac{1}{2}\,t)\; w\, f'_c} = \frac{2}{1.6 + C_M}\sqrt{\frac{3{,}000 \text{ p.s.i.}}{f'_c}} \quad (17)$$

Equation 17 may be obtained from equation 12 by setting $C_S = 1$.

Repeated Loading

The design equations 12 and 17 are based on tests and on strengths and allowable stresses relating only to short-time static loading. However, shear connectors in a bridge are subjected to repeated loading, and connectors located close to midspan are subjected to full reversal of stress for each passage of a vehicle. It is important, therefore, to determine whether a design based on equations 12 and 17 will be safe also from the standpoint of repeated loading.

The critical stresses at the design load may be computed from equations 12 or 17, and equations 1, 2, and 3. The absolute upper limit for the maximum stress in the concrete ($C_M = 0$, $C_S = 1$) may be expressed as:

$$\frac{f_{co}}{f'_c} = 1.25\sqrt{\frac{3{,}000 \text{ p.s.i.}}{f'_c}} \quad (18)$$

and the upper limit for the maximum stress in the steel may be expressed as:

$$f_{max} = \frac{1.25\, f'_c}{k_1}\sqrt{\frac{3{,}000 \text{ p.s.i.}}{f'_c}} \quad (19)$$

Since both of these critical stresses are functions solely of the cylinder strength of the concrete, their magnitude may easily be evaluated for the practical range of variables. This was done and the results are compared with safe values for repeated loading in figure 6.

In figure 6A the values computed from equation 18 are compared with the results of repeated load tests of small-scale composite T-beams (ref. *4B*). In the majority of these tests the dimensions of the channels were such that equation 1 for the maximum pressure on the concrete was applicable. Thus the pressure on the concrete could be evaluated and the fatigue strength of the connectors determined in terms of f_{co}/f'_c. This has been done for specimens failing at 600,000 repetitions of load or less (ref. *5*) and the limiting curve obtained from these studies is included in figure 6A. It should be mentioned, however, that with the possible exception of concrete strengths in the neighborhood of 2,000 p.s.i., the fatigue failure occurred in the channels and not in the concrete. In other words, the fatigue strength of the concrete adjacent to the channel was even higher than that indicated in figure 6A.

The fatigue strength of the channel shear connectors in terms of the maximum steel stress could not be determined from the small-scale experiments, since the dimensions of these specimens were such that equation 2 was not strictly

Table 3.—Relative efficiency of channel shear connectors

Channel type and size	Dimensions[1]			Relative efficiency of channels[2]
	$h + \frac{1}{2}\,t$	h	h'	
	In.	*In.*	*In.*	*Percent*
AMERICAN STANDARD:				
3-inch:				
4.1-lb.	0.462	0.377	0.170	100
5.0-lb.	.506	.377	.170	90
6.0-lb.	.555	.377	.170	82
4-inch:				
5.4-lb.	.503	.413	.180	82
7.25-lb.	.573	.413	.180	70
5-inch:				
6.7-lb.	.545	.450	.190	72
9.0-lb.	.613	.450	.190	62
6-inch:				
8.2-lb.	.587	.487	.200	63
10.5-lb.	.644	.487	.200	54
13.0-lb.	.706	.487	.200	48
7-inch:				
9.8-lb.	.628	.523	.210	57
12.25-lb.	.680	.523	.210	48
14.75-lb.	.733	.523	.210	44
CAR BUILDING:				
3-inch:				
7.1-lb.	.546	.390	.313	68
9.0-lb.	.640	.390	.313	63
4-inch:				
13.8-lb.	.781	.531	.469	50
SHIP BUILDING:				
6-inch:				
12.0-lb.	.570	.413	.337	42
15.1-lb.	.678	.521	.429	38
15.3-lb.	.610	.440	.330	35
16.3-lb.	.708	.521	.429	38
18.0-lb.	.717	.530	.420	35
7-inch:				
17.6-lb	.708	.521	.429	36
19.1-lb.	.729	.554	.446	34
22.7-lb.	.804	.554	.446	31

[1] Dimensions h, h', and t are shown in figure 2.
[2] Expressed as a percentage of the capacity of the 3-in., 4.1-lb. channel.

applicable. Therefore, the values computed from equation 19 are compared in figure 6B with the allowable steel stress for full reversal of loading (ref. *1*).

It can be concluded from the comparisons shown in figure 6 that connectors designed according to equations 12 or 17 will be safe from the standpoint of repeated loading.

Spacing and Cover

Spacing

The design load for a shear connector computed from equation 7 should not exceed the capacity of the connector given by equations 12 or 17. Thus, for a known size of channel, the required spacing s may be evaluated from equations 7 and 12 or 17. Since the maximum vertical design shear V_{des} varies along the lengths of the beam, and since it would seldom be advisable to vary the size of the connectors, the spacing of the connectors obtained by this procedure will vary along the beam.

A shear connector is required not only to transfer the horizontal shear from the slab to the beam but also to tie the slab and the beam together in the vertical direction. If the spacing of the connectors is not excessive, the upper flange of the channel provides an effective tie-down. The tests of full-size composite T-beams indicated that a spacing of 18 inches, equal to three times the thickness of the slab, was satisfactory, whereas a spacing of 36 inches, equal to six times the thickness of the slab, was unsatisfactory from the standpoint of vertical tie-down (ref. *6J*). It is recommended that the maximum spacing of channel shear connectors be not greater than four times the thickness of the slab, but in no case greater than 24 inches.

Cover

The concrete adjacent to the channel flange connected to the beam is subjected to localized high compressive stresses which can be sustained only if sufficient restraint is offered by the flange of the beam and by the surrounding concrete subjected to smaller stresses. It is important, therefore, that a sufficient cover of concrete be provided at the ends of the channel. It is believed that a 2-inch cover will offer the necessary restraint. (Some test data relating to this question may be found in ref. *6C*). For the same reason, the connector should be shorter than the width of the flange of the I-beam, and it is recommended that the connector should not extend closer than 1 inch to the edge of the beam flange —that is, the length of the connector should be at least 2 inches less than the width of the flange. Furthermore, if the slab is built with a concrete fillet between the I-beam and the main body of the slab, the width of this fillet should be at least 4 inches more than the length of the connector.

If the slab is built with a concrete fillet between the I-beam and the main body of the slab, shearing stresses of considerable magnitude exist in this fillet. It is desirable, therefore, that the connectors extend some distance into the main body of the slab. It is recommended that this distance be at least 2 inches, and preferably 3 inches.

Design of Connecting Welds

The most common method of connecting a shear connector to the top flange of an I-beam is by welding. In all tests made at the University of Illinois, the connection was made by continuous welds extending the full width of the channel at both the heel and toe.

Static loading

Tests of individual shear connectors indicated that the ultimate strength of the welded connection may be estimated as the product of the throat area of the welds and 80,000 p.s.i. (ref. *6C*). The allowable stress specified by the current specifications (ref. *2*) is 12,400 p.s.i. Thus the factor of safety against failure of welds designed for the allowable stress and for the full load capacity of the connector is 6.4 at working loads, and at least 2.4 at first yielding of the connectors. Since the ratio of the ultimate strength to the yield strength of the connector itself varies approximately from 2.0 to 3.0 (table 1), the corresponding minimum value of 2.4 for welds seems to be reasonable. Thus, the effective area of the welds for shear connectors may be computed as:

$$A_w \geq \frac{Q_{des}}{12{,}400 \text{ p.s.i.}} \qquad (20)$$

Repeated loading

Current specifications (ref. *2*) require that the effective area of welds subject to repeated loading be:

$$A_w \geq \frac{\text{Max. } Q - \frac{1}{2} \text{ Min. } Q}{10{,}000 \text{ p.s.i.}} \qquad (21)$$

In this formula the terms "Max." and "Min." refer to the maximum and minimum loads on shear connectors. "Max." refers to the numerically greater load and should always be taken as a plus quantity. If the minimum load has opposite direction to that of the maximum load, the "Min." should be taken as a minus quantity. The magnitudes of the Max. Q and Min. Q should be computed from equation 7; in this equation V should be the maximum or minimum shear caused by that portion of the design loads acting on the bridge which contributes to the load acting on shear connectors, and s the actual spacing of the shear connectors.

Size of welds

The maximum allowable size of welds is governed by the dimensions of the channel. The weld on the front of the channel cannot be higher than the minimum thickness of the channel flange, h' (fig. 2). The height of the weld on the back of the channel is also limited since it is undesirable for the weld to extend to the section of maximum steel stresses in the channel. It is recommended, therefore, that the weld on the back of the channel be always at least one-eighth inch lower than h. Values of h and h' for various channels are listed in table 3.

Relative Efficiency of Channels of Various Sizes

The load-carrying capacity of a channel shear connector is proportional to the sum of the maximum flange thickness h and one-half of the web thickness t (equations 12 and 17). Thus the contribution of the web to the load-carrying capacity of the connector is relatively small. Furthermore, the capacity is independent of the depth of the channel. Since the value of h for rolled channels varies only from 0.377 inch for the lightest to 0.554 inch for the heaviest types suitable for shear connectors, it may be expected that from the standpoint of steel economy alone the lightest channels will be the most efficient. This point is illustrated in table 3.

In the last column of table 3, termed "Relative efficiency of channels," the relative load-carrying capacity per pound of steel in the channel is listed for various channels as a percentage of the capacity of the lightest channel. It is evident from this table that the efficiency generally decreases with increasing weight, whereas for any particular depth of channel the lightest channel is the most efficient.

The load-carrying capacity of a channel connector increases also with increasing strength of concrete. In practical design, however, the strength of concrete is governed by other considerations and for the design of connectors is a fixed quantity. Thus the designer will generally

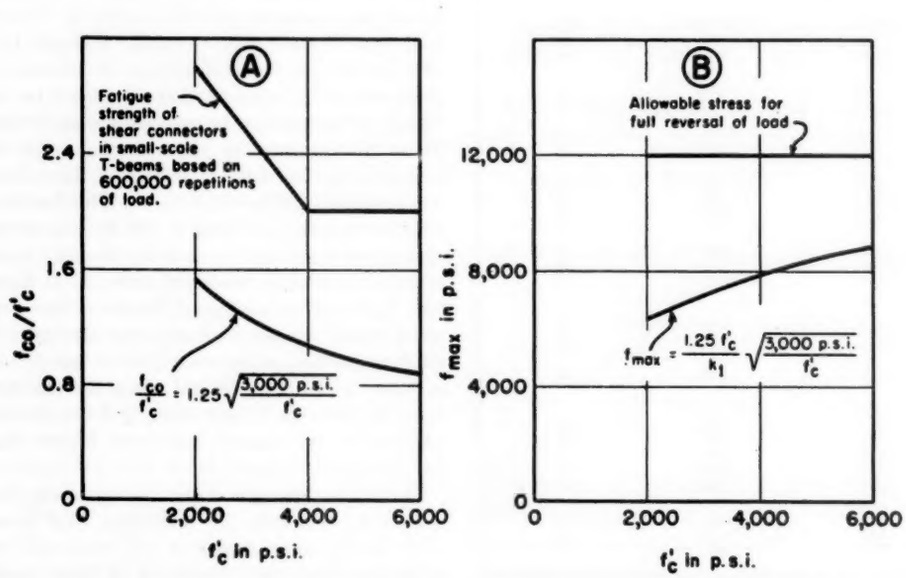

Figure 6.—Variation of f_{co}/f'_c and f_{max} with concrete strength at design load.

be able to vary the capacity of the connector only by varying the dimensions and the spacing of the connectors.

Concluding Remarks

The procedure for the design of channel shear connectors presented in this article is based on the assumption that all of the horizontal shear at the junction between the concrete slab and the steel I-beams is transferred through the shear connectors. At working loads this assumption may be overly conservative since bond may exist between the two elements. If bond is present initially, there is some evidence from both field and laboratory that the presence of strong shear connectors can prevent the destruction of this bond under service conditions. It is unlikely, however, that the bond would survive any serious overstress of the structure, and once the bond is broken it cannot be restored. It is therefore the opinion of the authors that the mechanical shear connectors should be designed for full horizontal shear.

The tests of small-scale T-beams have demonstrated that the presence of bond increases substantially the fatigue life of the shear connectors (ref. *4C*). All specimens tested in fatigue were built with shear connectors, and in most specimens the bond between the steel beam and the concrete slab was broken before the fatigue test was begun, with the result that all of the horizontal shear was carried by the shear connectors. In a few specimens, however, the bond failed only during the fatigue tests; and in two specimens the bond remained unbroken throughout the tests. These specimens with bond withstood more repetitions of load than the corresponding specimens without bond, and the two specimens in which the bond did not break at all withstood over 2,000,000 repetitions of load without any signs of damage. Since it is most probable that bond exists in actual structures, at least for some time, it might be possible to relax the design requirements based on repeated loading. It can be seen from the previous paragraphs that such a provision would affect only the design of welds.

The analysis on which the design procedure is based contains empirical parameters determined from the tests of channel shear connectors. Consequently, the use of this procedure must be limited to channel shear connectors within the range of variables included in the tests. Fortunately, the range of variables in the tests was great enough to accommodate all channels deeper than 3 inches. It is possible that the procedure might be applicable also to some other rolled steel shapes. However, any such extension of the applicability of the procedure would have to be substantiated by tests.

The procedure for the design of channel shear connectors and its limitations may be summarized as follows:

1. For composite beams built without temporary supports, flexible channel shear connectors made of structural steel and attached to wide-flange beams made of structural steel may be designed according to equation 12.
2. For composite beams built with temporary supports, channels made of structural steel attached to wide-flange beams made of structural steel may be designed according to equation 17.
3. The spacing of the connectors should be determined from equation 7, and should not be greater than four times the slab thickness, or 24 inches.
4. The length of channel connectors should not be greater than the width of the supporting flange of the I-beam minus 2 inches.
5. If the slab is built with a concrete fillet between the I-beam and the main body of the slab, the width of the fillet should be at least 4 inches more than the length of the connectors. The connectors should extend at least 2 inches above the bottom of the main body of the slab.

REFERENCES

(*1*) American Association of State Highway Officials
Standard specifications for highway bridges. American Association of State Highway Officials, Washington, D. C., 1949, art. 3.6.5.

(2) American Welding Society
Standard specifications for welded highway and railway bridges. American Welding Society, New York, 1947.

(3) Siess, C. P.
Composite construction for I-beam bridges. Transactions of the American Society of Civil Engineers, New York, vol. 114, 1949, pp. 1023-1045.

(*4*) Siess, C. P., Viest, I. M., and Newmark, N. M.
Studies of slab and beam highway bridges, part III: Small-scale tests of shear connectors and composite T-beams. University of Illinois Engineering Experiment Station Bulletin No. 396, Urbana, 1952.

(*4A*) *Bulletin 396,* section 25, pp. 63-71.

(*4B*) *Bulletin 396,* chapter V, pp. 81-109.

(*4C*) *Bulletin 396,* section 35, pp. 91-95.

(*5*) Viest, I. M.
Full-scale tests of channel shear connectors and composite T-beams. A Ph. D. thesis, University of Illinois, Urbana, 1951, section 44, pp. 113-116.

(*6*) Viest, I. M., Siess, C. P., Appleton, J. H., and Newmark, N. M.
Studies of slab and beam highway bridges, part IV: Full-scale tests of channel shear connectors and composite T-beams. University of Illinois Engineering Experiment Station Bulletin No. 405, Urbana, 1952.

(*6A*) *Bulletin 405,* table 5, pp. 26-27.

(*6B*) *Bulletin 405,* section 12, pp. 28-45.

(*6C*) *Bulletin 405,* section 15, pp. 53-55.

(*6D*) *Bulletin 405,* section 27, pp. 74-76.

(*6E*) *Bulletin 405,* section 28, pp. 76-78.

(*6F*) *Bulletin 405,* sections 38-41, pp. 98-118.

(*6G*) *Bulletin 405,* table 24, p. 116.

(*6H*) *Bulletin 405,* section 42, pp. 118-123.

(*6J*) *Bulletin 405,* section 44, pp. 124-126.

ILLUSTRATIVE EXAMPLE

Basic information

Span of beams: 60 ft.
Beam spacing: 6 ft.
For effective slab width, see A.A.S.H.O. Specifications, 1949, Art. 3.9.2.
Structural grade steel.
Concrete strength: 3,000 p.s.i.
Beams not shored during construction.
Loading: H20-S16-44.
Allowable stresses (A.A.S.H.O. Specifications, 1949, revised 1950):

Steel: $f_s = 18{,}000$ p.s.i.
Concrete: $f_c = 1{,}200$ p.s.i.
$n = 10$.

Cross-section of T-beam:

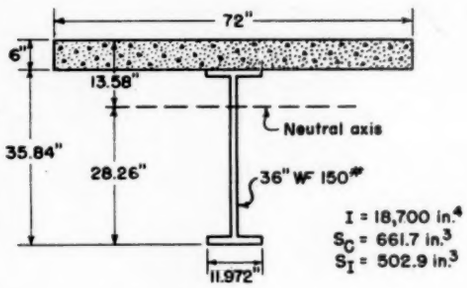

Design of shear connectors

Horizontal shear (equation 7):

$$\frac{Q_{des}}{s} = \frac{V\ 72 \times 6\ (13.58 - 3.00)}{10 \times 18{,}700} = 0.0244\ V.$$

Vertical shear at end:

$$V = (16{,}000 + \frac{6.0}{5.5}16{,}000\frac{60-14}{60} + \frac{6.0}{5.5}4{,}000\frac{60-28}{60})(1 + \frac{50}{60+125}) = 40{,}300 \text{ lb.}$$

Vertical shear 12 ft. from end:

$$V = \frac{6.0}{5.5}(16{,}000\frac{60-12}{60} + 16{,}000\frac{60-12-14}{60} + 4{,}000\frac{60-12-2\times14}{60}$$

$$(1 + \frac{50}{60-12+125}) = 32{,}600 \text{ lb.}$$

Vertical shear 24 ft. from end:

$$V = \frac{6.0}{5.5}(16{,}000\frac{60-24}{60} + 16{,}000\frac{60-24-14}{60} + 4{,}000\frac{60-24-2\times14}{60}) \times 1.3 = 22{,}700 \text{ lb.}$$

Use 3-in., 4.1-lb channel of maximum allowable length $w = 11.97 - 2 \doteq 10$ in.
From table 3: $h + \frac{1}{2}t = 0.462$.
From the design of beams:

$$C_M = \frac{M_{DL}}{M_{LL}} = 0.483;\ C_S = \frac{S_C}{S_I} = 1.316.$$

From equation 12:

$$Q_{des} = \frac{0.462 \times 10 \times 3{,}000}{0.8 + (0.8 \times 1.316 - 0.3)\ 0.483}\sqrt{\frac{3{,}000}{3{,}000}} = 11{,}910 \text{ lb.}$$

Spacing at end:

$$s = \frac{11{,}910}{0.0244 \times 40{,}300} = 12.1 \text{ in.}$$

Spacing 12 ft. from end:

$$s = \frac{11{,}910}{0.0244 \times 32{,}600} = 15.0 \text{ in.}$$

Spacing 24 ft. from end:

$$s = \frac{11{,}910}{0.0244 \times 22{,}700} = 21.6 \text{ in.}$$

Spacing diagram:

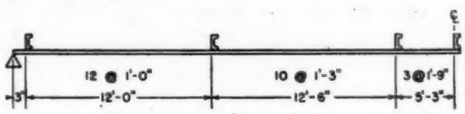

Connecting welds

Weld area required at end:

$V_{max} = 40{,}300$ lb.; $V_{min} = 0$.

From equation 7: $Q_{max} = 0.0244 \times 40{,}300 \times 12 = 11{,}800$ lb.; $Q_{min} = 0$.

$$A \geq \frac{11{,}800}{10{,}000} = 1.18 \text{ in.}^2$$

Weld area required 12 ft. from end:

$V_{max} = 32{,}600$ lb.;

$$V_{min} = \frac{6.0}{5.5}(16{,}000\frac{60-12}{60} - 16{,}000) \times 1.3 = -4{,}540 \text{ lb.}$$

$Q_{max} = 0.0244 \times 32{,}600 \times 15 = 11{,}930$ lb.
$Q_{min} = -0.0244 \times 4{,}540 \times 15 = -1{,}660$ lb.

$$A \geq \frac{11{,}930 + \frac{1}{2}\ 1{,}660}{10{,}000} = 1.28 \text{ in.}^2$$

Weld area required 24 ft. from end:

$V_{max} = 22{,}700$ lb.

$$V_{min} = \frac{6.0}{5.5}(16{,}000\frac{60-24}{60} + 16{,}000\frac{60-24+14}{60} - 2 \times 16{,}000) \times 1.3 = -12{,}860 \text{ lb.}$$

$Q_{max} = 0.0244 \times 22{,}700 \times 21 = 11{,}630$ lb.
$Q_{min} = -0.0244 \times 12{,}860 \times 21 = -6{,}590$ lb.

$$A \geq \frac{11{,}630 + \frac{1}{2}\ 6{,}590}{10{,}000} = 1.49 \text{ in.}^2$$

Weld area required at midspan:

$$V_{max} = -V_{min} = \frac{6.0}{5.5}(16{,}000\frac{60-30}{60} + 16{,}000\frac{60-30-14}{60} + 4{,}000\frac{60-30-2\times14}{60}) \times 1.3 = 17{,}590 \text{ lb.}$$

$$Q_{max} = -Q_{min} = 0.0244 \times 17{,}590 \times 21 = 9{,}010 \text{ lb.}$$

$$A \geq \frac{9{,}010 + \frac{1}{2}\ 9{,}010}{10{,}000} = 1.35 \text{ in.}^2$$

Area available with $\frac{3}{16}$-in. weld at the heel and toe of channel,

$A = 0.707 \times \frac{3}{16} \times 2 \times 10 = 2.65$ in.^{2}, is sufficient.

A list of the more important articles in PUBLIC ROADS may be obtained upon request addressed to Bureau of Public Roads, Washington 25, D. C.

PUBLICATIONS of the Bureau of Public Roads

The following publications are sold by the Superintendent of Documents, Government Printing Office, Washington 25, D. C. Orders should be sent direct to the Superintendent of Documents. Prepayment is required.

ANNUAL REPORTS

Work of the Public Roads Administration:

1941, 15 cents. 1948, 20 cents.
1942, 10 cents. 1949, 25 cents.

Public Roads Administration Annual Reports:

1943; 1944; 1945; 1946; 1947. (*Free from Bureau of Public Roads*)

Annual Reports of the Bureau of Public Roads:

1950, 25 cents. 1952, 25 cents.
1951, 35 cents. 1953, 25 cents.

HOUSE DOCUMENT NO. 462

Part 1.—Nonuniformity of State Motor-Vehicle Traffic Laws (1938). 15 cents.

Part 2.—Skilled Investigation at the Scene of the Accident Needed to Develop Causes (1938). 10 cents.

Part 3.—Inadequacy of State Motor-Vehicle Accident Reporting (1938). 10 Cents.

Part 4.—Official Inspection of Vehicles (1938). 10 cents.

Part 5.—Case Histories of Fatal Highway Accidents (1938). 10 cents.

Part 6.—The Accident-Prone Driver (1938). 10 cents.

UNIFORM VEHICLE CODE

Act I.—Uniform Motor-Vehicle Administration, Registration, Certificate of Title, and Antitheft Act (1945). 15 cents.

Act II.—Uniform Motor-Vehicle Operators' and Chauffeurs' License Act (revised 1952). 15 cents.

Act III.—Uniform Motor-Vehicle Civil Liability Act (1944). 10 cents.

Act IV.—Uniform Motor-Vehicle Safety Responsibility Act (revised 1952). 15 cents.

Act V.—Uniform Act Regulating Traffic on Highways (revised 1952). 20 cents.

Model Traffic Ordinance (revised 1952). 20 cents.

MAPS

State Transportation Map series (available for 39 States). Uniform sheets 26 by 36 inches, scale 1 inch equals 4 miles. Shows in colors Federal-aid and State highways with surface types, principal connecting roads, railroads, airports, waterways, National and State forests, parks, and other reservations. Prices and number of sheets for each State vary—see Superintendent of Documents price list 53.

United States System of Numbered Highways together with the Federal-Aid Highway System (also shows in color National forests, parks, and other reservations). 5 by 7 feet (in 2 sheets), scale 1 inch equals 37 miles. $1.25.

United States System of Numbered highways. 28 by 42 inches, scale 1 inch equals 78 miles. 20 cents.

MISCELLANEOUS PUBLICATIONS

Bibliography of Highway Planning Reports (1950). 30 cents.

Construction of Private Driveways, No. 272MP (1937). 15 cents.

Design Capacity Charts for Signalized Street and Highway Intersections (reprint from PUBLIC ROADS, Feb. 1951). 25 cents.

Electrical Equipment on Movable Bridges, No. 265T (1931). 40 cents.

Factual Discussion of Motortruck Operation, Regulation, and Taxation (1951). 30 cents.

Federal Legislation and Regulations Relating to Highway Construction (1948). Out of print.

Financing of Highways by Counties and Local Rural Governments, 1931—41. 45 cents.

Highway Bond Calculations (1936). 10 cents.

Highway Bridge Location, No. 1486D (1927). 15 cents.

Highway Capacity Manual (1950). 75 cents.

Highway Needs of the National Defense, House Document No. 249 (1949). 50 cents.

Highway Practice in the United States of America (1949). 75 cents.

Highway Statistics (annual):

1945, 35 cents. 1948, 65 cents. 1951, 60 cents.
1946, 50 cents. 1949, 55 cents. 1952, 75 cents.
1947, 45 cents. 1950 (out of print).

Highway Statistics, Summary to 1945. 40 cents.

Highways in the United States, *nontechnical* (1951). 15 cents.

Highways of History (1939). 25 cents.

Identification of Rock Types (1950). 10 cents.

Interregional Highways, House Document No. 379 (1944). 75 cents.

Legal Aspects of Controlling Highway Access (1945). 15 cents.

Local Rural Road Problem (1950). 20 cents.

Manual on Uniform Traffic Control Devices for Streets and Highways (1948). 75 cents.

Mathematical Theory of Vibration in Suspension Bridges (1950). $1.25.

Principles of Highway Construction as Applied to Airports, Flight Strips, and Other Landing Areas for Aircraft (1943). $2.00.

Public Control of Highway Access and Roadside Development (1947). 35 cents.

Public Land Acquisition for Highway Purposes (1943). 10 cents.

Results of Physical Tests of Road-Building Aggregate (1953). $1.00.

Roadside Improvement, No. 191MP (1934). 10 cents.

Selected Bibliography on Highway Finance (1951). 60 cents.

Specifications for Construction of Roads and Bridges in National Forests and National Parks, FP-41 (1948). $1.50.

Standard Plans for Highway Bridge Superstructures (1953). $1.00.

Taxation of Motor Vehicles in 1932. 35 cents.

Tire Wear and Tire Failures on Various Road Surfaces (1943). 10 cents.

Transition Curves for Highways (1940). $1.75.

Single copies of the following publications are available to highway engineers and administrators for official use, and may be obtained by those so qualified upon request addressed to the Bureau of Public Roads. They are not sold by the Superintendent of Documents.

Bibliography on Automobile Parking in the United States (1946).

Bibliography on Highway Lighting (1946).

Bibliography on Highway Safety (1938).

Bibliography on Land Acquisition for Public Roads (1947).

Bibliography on Roadside Control (1949).

Express Highways in the United States: a Bibliography (1945).

Indexes to PUBLIC ROADS, volumes 17–19 and 23.

Title Sheets for PUBLIC ROADS, volumes 24–27.

DEPARTMENT OF COMMERCE - BUREAU OF PUBLIC ROADS

STATUS OF FEDERAL-AID HIGHWAY PROGRAM

AS OF FEBRUARY 28, 1954

FOR OFFICIAL USE

(Thousand Dollars)

STATE	UNPROGRAMMED BALANCES	ACTIVE PROGRAM											
		PROGRAMMED ONLY			PLANS APPROVED, CONSTRUCTION NOT STARTED			CONSTRUCTION UNDER WAY			TOTAL		
		Total Cost	Federal Funds	Miles	Total Cost	Federal Funds	Miles	Total Cost	Federal Funds	Miles	Total Cost	Federal Funds	Miles
Alabama	$11,654	$12,717	$6,766	179.7	$8,373	$4,210	68.2	$45,021	$22,935	495.8	$66,111	$33,911	743.7
Arizona	3,362	7,959	5,643	177.9	1,009	645	9.0	5,363	3,810	68.5	14,331	10,098	255.4
Arkansas	9,399	8,046	4,722	316.7	7,100	3,543	161.6	10,600	5,334	246.1	25,746	13,599	724.4
California	16,596	24,031	12,462	152.4	13,377	6,918	31.2	86,540	41,499	203.0	123,948	60,879	386.6
Colorado	10,788	2,432	1,357	39.7	1,943	1,090	59.5	19,146	10,368	190.4	23,521	12,815	289.6
Connecticut	12,036	450	275	2.0	1,047	516	1.0	8,461	4,220	26.0	9,958	5,011	29.0
Delaware	3,205	3,756	1,905	23.1	1,404	699	11.9	3,603	1,797	18.8	8,763	4,401	53.8
Florida	12,168	12,748	6,418	162.1	4,813	2,546	91.5	20,533	10,741	307.7	38,094	19,705	561.3
Georgia	15,919	16,888	8,503	311.6	4,381	2,156	81.9	36,254	17,146	520.9	57,523	27,805	914.4
Idaho	2,916	12,705	8,025	270.2	3,091	1,886	42.8	10,242	6,372	172.2	26,038	16,283	485.2
Illinois	24,158	36,225	18,808	343.6	19,645	9,706	84.0	54,566	29,055	299.7	110,436	57,569	727.3
Indiana	12,416	48,681	25,714	240.1	13,897	6,967	92.2	16,413	8,718	54.8	78,991	41,399	387.1
Iowa	11,672	14,153	7,532	513.6	7,231	3,771	181.7	13,657	7,637	454.6	35,041	18,940	1,149.9
Kansas	10,461	14,546	7,270	938.5	4,544	2,368	259.2	12,947	6,320	665.0	32,037	15,958	1,862.7
Kentucky	10,510	9,351	5,017	108.9	7,104	3,555	91.4	21,136	11,084	203.7	37,591	19,656	404.0
Louisiana	8,407	21,635	10,063	155.8	5,102	2,546	43.1	25,483	12,338	113.8	52,220	24,947	312.7
Maine	5,254	4,252	2,149	30.9	1,164	563	4.9	11,197	5,611	84.7	16,516	8,323	120.5
Maryland	8,358	13,435	7,083	46.2	2,869	1,501	19.4	9,866	5,406	33.3	26,170	13,990	98.9
Massachusetts	8,483	2,897	1,583	6.1	13,231	6,566	13.3	42,346	19,679	28.2	58,474	27,828	47.6
Michigan	19,443	26,169	13,154	415.5	6,922	3,724	126.5	36,217	16,861	200.4	69,308	33,739	742.4
Minnesota	15,002	9,410	5,203	804.9	6,186	3,196	152.1	12,789	6,760	201.8	28,385	15,159	1,158.8
Mississippi	7,910	12,442	6,337	332.8	4,988	2,464	161.9	19,536	9,862	448.2	36,966	18,663	942.9
Missouri	15,915	18,032	9,385	814.4	7,960	4,058	184.6	47,141	23,134	365.6	73,133	36,577	1,364.6
Montana	6,570	20,298	12,310	603.2	4,227	2,530	98.1	17,731	10,703	260.2	42,256	25,543	961.5
Nebraska	14,796	18,882	9,888	647.7	9,733	5,082	212.9	7,426	4,304	211.0	36,041	19,274	1,071.6
Nevada	7,035	2,727	2,283	96.0	2,441	2,027	21.5	6,015	4,993	111.8	11,183	9,303	229.3
New Hampshire	3,108	5,174	2,587	34.7	1,226	603	2.9	5,153	2,667	31.3	11,553	5,857	68.9
New Jersey	10,535	13,694	4,322	51.9	4,865	2,323	9.7	24,425	11,776	17.8	42,984	18,421	79.4
New Mexico	5,254	4,110	2,552	133.7	2,412	1,528	51.3	10,072	6,291	224.2	16,594	10,371	409.2
New York	38,618	71,118	37,296	257.8	45,386	22,144	42.2	136,794	64,086	343.4	253,298	123,526	643.4
North Carolina	13,668	19,761	9,835	483.5	5,105	2,264	98.4	32,865	15,722	394.9	57,731	27,821	976.8
North Dakota	3,342	12,062	6,047	1,228.5	4,738	2,369	288.7	6,501	3,403	336.9	23,301	11,819	1,854.1
Ohio	23,784	8,966	4,918	56.8	19,047	8,001	65.6	78,078	37,245	94.0	106,091	50,164	216.4
Oklahoma	15,009	11,928	6,621	135.1	7,498	3,959	139.8	13,635	7,433	177.4	33,061	18,013	452.3
Oregon	5,627	4,266	2,548	36.6	3,720	2,035	43.0	10,576	6,457	148.0	18,562	11,040	227.6
Pennsylvania	13,220	43,304	20,358	82.3	11,209	5,069	32.7	95,291	46,577	177.8	149,804	72,004	292.8
Rhode Island	4,684	2,952	1,476	40.2	307	153		9,847	4,921	24.6	13,106	6,550	64.8
South Carolina	6,943	12,707	6,990	366.3	2,555	1,287	141.1	15,090	7,461	351.8	30,352	15,738	859.2
South Dakota	2,096	15,445	8,854	815.6	1,817	1,019	97.0	6,967	3,891	377.1	24,229	13,764	1,289.7
Tennessee	12,029	12,336	6,146	500.9	9,305	4,664	260.2	30,631	13,965	250.4	52,272	24,775	1,011.5
Texas	30,721	11,061	5,806	206.9	11,732	6,033	235.7	54,981	29,601	1,024.0	77,774	41,440	1,466.6
Utah	953	8,416	6,363	171.0	1,384	1,038	25.6	8,842	6,783	128.6	18,642	14,184	325.2
Vermont	2,153	3,883	1,942	44.0	830	415	9.2	6,519	3,303	35.7	11,232	5,660	88.9
Virginia	9,479	8,253	3,898	78.7	6,811	3,054	103.8	30,291	14,543	194.6	45,355	21,495	377.1
Washington	5,349	17,028	8,514	242.9	1,925	1,025	27.5	16,839	8,917	106.0	35,792	18,456	376.4
West Virginia	9,043	7,101	3,599	48.5	5,332	2,677	12.3	10,149	5,038	45.7	22,582	11,314	106.5
Wisconsin	6,965	24,054	12,431	313.8	2,525	1,331	85.0	23,130	11,546	192.2	49,709	25,308	591.0
Wyoming	1,708	6,846	4,447	216.7	934	605	22.1	7,717	4,842	137.4	15,497	9,894	376.2
Hawaii	3,211	2,111	1,026	3.2	1,858	924	3.5	9,810	4,677	14.3	13,779	6,627	21.0
District of Columbia	4,160	7,368	3,444	5.5	153	71		12,604	5,814	3.0	20,125	9,329	8.5
Puerto Rico	7,092	10,339	4,762	50.3	652	315	4.0	14,727	6,865	39.9	25,718	11,942	94.2
TOTAL	524,724	719,053	376,637	13,339.0	317,108	159,739	4,106.7	1,271,763	640,511	10,857.2	2,307,924	1,176,887	28,302.9

U. S. GOVERNMENT PRINTING OFFICE 72196